Geophys. J. Int. (2003) **152,** 372–391

Crustal structure across the Canadian High Arctic region from teleseismic receiver function analysis

Fiona A. Darbyshire

National Earthquake Hazards Program, Geological Survey of Canada, 7 Observatory Crescent, Ottawa, ON, K1A 0Y3, *Canada.*
E-mail: fiona@seismo.nroan.go.ca

Accepted 2002 August 6. Received 2002 July 29; in original form 2002 March 4

SUMMARY

Results from an investigation of the crustal structure beneath the Canadian High Arctic and western Greenland are presented, using teleseismic data recorded by a network of 12 three-component broad-band seismograph stations deployed across the region. Of these stations, eight were deployed in summer 2000, in order to improve the spatial density of seismographs in this tectonically active but little studied region, in order to provide more information on the patterns of seismicity and the structure of the area. The typical station separation is of the order of 400–600 km, a substantial improvement on the previous >1000 km spacing afforded by the permanent broad-band network. Teleseismic receiver functions are used to model the shear wave velocity structure of the crust beneath the stations, using both 1-D and 3-D analysis techniques.

The velocity–depth models show significant variation in the thickness and nature of the crust across the region. In the south and east, where the seismic stations lie on the Canadian Shield, the crustal structure is relatively simple, with Moho depths ranging from 35 km on the Boothia Peninsula to 45 km beneath southern Baffin Island.

Further to the north and west, where the lithosphere has been deformed by orogenic events and basin formation, the patterns of azimuthal variation in the radial and tangential receiver functions suggest 3-D structure throughout the crust. The Moho depths around the margins of the Sverdrup Basin lie in the range 33–37 km. At Mould Bay, on the western margin of the basin, a 5 km thick low-velocity layer overlies the main crustal sequence. The base of this layer can be modelled as a planar dipping structure with a southeasterly strike. The thinnest crust (27–32 km) is modelled at Alert, on the northern coast of Ellesmere Island.

In the southwest of the Arctic archipelago, tangential receiver functions at Holman show a pattern consistent with crustal anisotropy. The Moho depth in the region is undetermined; a layer of intermediate shear wave velocity, consistent with mafic lower-crustal material, is modelled at depths of 35–55 km. The region around Holman lies at the focal point of the Mackenzie dyke swarm, believed to result from plume activity; therefore the intermediate-velocity layer may result from mafic underplating caused by the presence of the Mackenzie plume.

Key words: Canadian Arctic, crustal structure, receiver functions.

1 INTRODUCTION

The Canadian High Arctic region is complex, with several episodes of geosynclinal and orogenic development shaping the lithospheric structure since the Late Proterozoic (Kerr 1977; Trettin 1991). The northern mainland area and Baffin Island are dominated by sub-provinces of the Canadian Shield, but much of the archipelago is characterized by Phanerozoic geological provinces (Fig. 1).

The northern Canadian Shield consists of Archaean and Proterozoic structures, consisting of a set of Archaean provinces bounded by younger magmatic arcs, suture zones and fold belts (e.g. Lewry & Collerson 1990; Hoffman 1990). Most of the Shield rocks in the area of interest to this study lie within the Rae province and its neighbouring fold belts, the exception being the Precambrian outcrops of the Minto Arch on Victoria Island, which are an uplifted section of the Bear Province, flanked by Palaeozoic sediments.

The Shield provinces are thought to have been amalgamated between 1.97 and 1.82 Ga (Hoffman 1990). One of the major orogens contributing to the structure of the Shield, and of interest to this study, is the Early Proterozoic Trans-Hudson Orogen, which extends northeastwards from South Dakota, through Saskatchewan and Manitoba and across Hudson Bay (e.g. Lewry & Collerson 1990), and is now

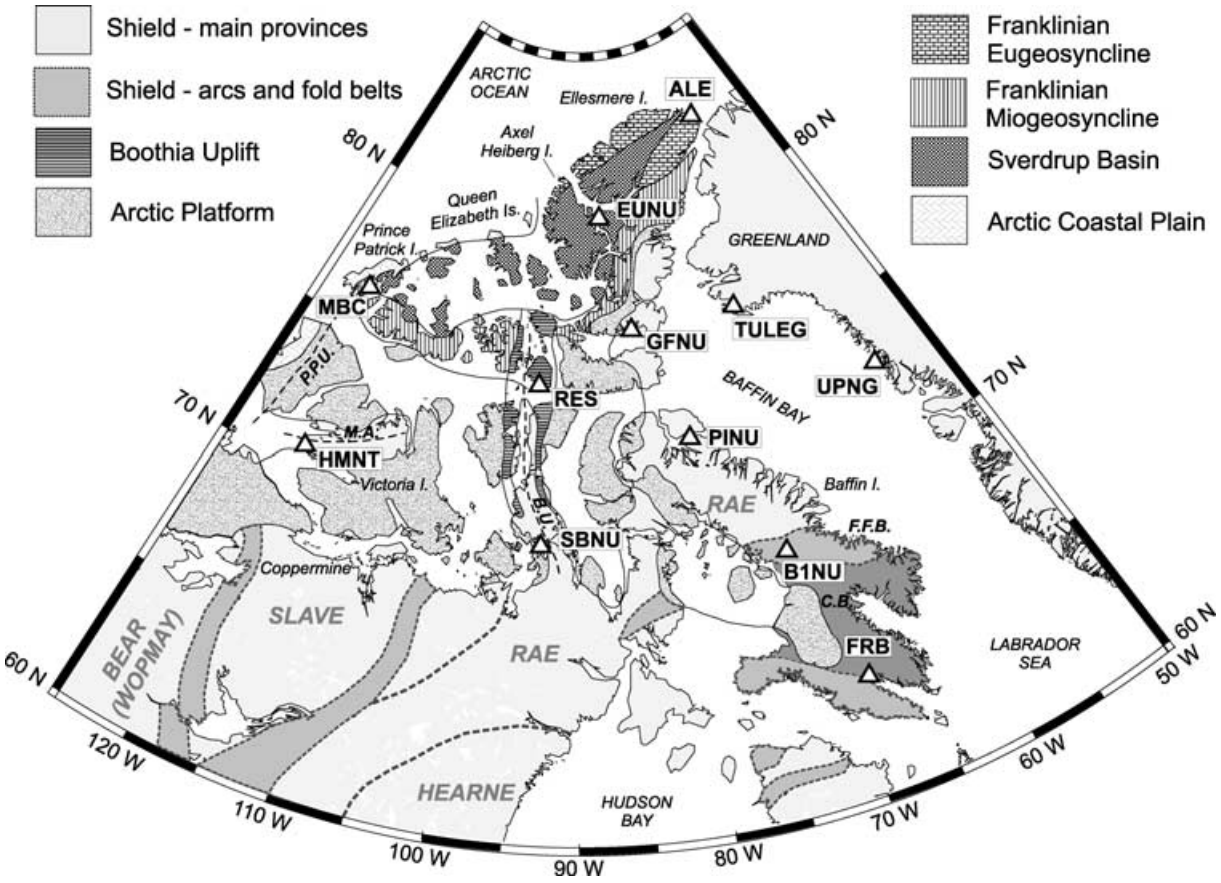

Figure 1. Map of the Canadian High Arctic region, showing major geological provinces (after Thorsteinsson & Tozer 1970; Hoffman 1990; Lewry & Collerson 1990). Broad-band seismic stations used in this study are shown as white triangles. P.P.U., Prince Patrick Uplift; M.A., Minto Arch; B.U., Boothia Uplift; F.F.B., Foxe Fold Belt; C.B., Cumberland Batholith. Names written in grey italics are geological provinces of the Canadian Shield and dashed lines show the boundaries between these provinces.

considered to extend across the southern half of Baffin Island and into western Greenland (e.g. Corrigan *et al.* 2001).

Northern Baffin Island has been recognized for some time as an eastward extension of the Rae province (Hoffman 1988), made up of reworked Archaean material of age >2.7 Gyr. To the south, in central Baffin Island, the rocks of the Piling Group delineate the Foxe Fold Belt, which makes up the northern margin of the Trans-Hudson Orogen. South of the Foxe Fold Belt, and bounded by two other major fold belts, is the Cumberland Batholith, emplaced at ∼1.86 Ga (Corrigan *et al.* 2001). The southern half of Baffin Island has been extensively deformed; evidence can be seen in the form of igneous intrusions, tight folds and fold interference patterns (e.g. Hoffman 1988; Corrigan *et al.* 2001).

The most northerly section of the Canadian Shield exposed on the mainland is the Boothia Uplift, which was formed between the Late Proterozoic and the Late Devonian by episodic pulses of tectonic uplift, and later fragmented during the Eurekan deformation period in the Cretaceous and Tertiary (Kerr 1977; Okulitch *et al.* 1991). The Boothia Uplift plunges to the north and disappears beneath younger rocks, though structures arising from the uplift and folding can be seen further north as the Cornwallis Fold Belt and Cornwall Arch, between ∼74° and 78° north. The major part of the uplift coincided with the closing pulses of the Caledonian Orogeny, and may have occurred in response to associated compressional stresses (Okulitch *et al.* 1991).

The Arctic Lowlands (or Arctic Platform), a region of little-disturbed Palaeozoic rocks, dominates much of the southern part of the Arctic archipelago. Further north, a complex fold belt resulting from the Ellesmerian Orogeny in the Late Devonian to Early Carboniferous produces the structures of the Franklinian Geosyncline (Thorsteinsson & Tozer 1970; Trettin 1991).

In the northern Arctic archipelago, the major geological province is the Sverdrup Basin, which lies on top of the deformed Franklinian Geosyncline and is bounded to the southwest, northeast and east by Franklinian fold belts. The basin is made up of a thick sedimentary succession, up to ∼15 km deep, deposited between the lower Carboniferous and the Late Cretaceous (e.g. Forsyth *et al.* 1979). Northeast-trending features such as faults, linear magnetic anomalies, gabbroic dykes and aligned evaporite domes suggest that the Sverdrup Basin represents an incipient rift in the margin of the North American continent, with a long history of crustal instability (Balkwill & Fox 1982). The tectonic architecture of the region was also reorganized by lithospheric extension connected to the opening of the Labrador Sea/Baffin Bay rift system in the Early Cretaceous, and by the Eurekan orogenic episode in the Late Cretaceous to Early Tertiary (Forsyth *et al.* 1979; Balkwill & Fox 1982; Ziegler 1988; Trettin 1991).

The northernmost margins of the Arctic islands are characterized by Cretaceous and Cenozoic sediments, representing the landward side of the Arctic continental rifted margin.

Table 1. Seismic stations in the High Arctic region for which receiver function analysis was carried out. For locations: NU, Nunavut Territory; NWT, Northwest Territories. 'Type' denotes the station network. IRIS, run by the Incorporated Research Institutions for Seismology; CNSN, Canadian National Seismograph Network; CHASME, Canadian High Arctic Seismic Monitoring Experiment; CGD, Operated by the Continental Geoscience Division of the Geological Survey of Canada. Negative longitudes represent degrees west. Note that the final column shows the time period (years) from which teleseismic data were used in this study. With the exceptions of GFNU, UPNG and MBC, the stations are still in operation.

Station name	Location	Type	Latitude	Longitude	Time period of data used
ALE	Alert, NU	IRIS	82.5033	−62.3500	1992–1999
FRB	Iqaluit, NU	CNSN	63.7467	−68.5467	1993–2000
MBC	Mould Bay, NWT	CNSN	76.2417	−119.3600	1993–1997
RES	Resolute, NU	CNSN	74.6870	−94.9000	1995–2000
B1NU	Baffin Island, NU	CGD	68.4619	−71.5880	2000–2001
EUNU	Eureka, NU	CHASME	80.0533	−86.4158	2000–2001
GFNU	Grise Fiord, NU	CHASME	76.4177	−82.9006	2000–2001
HMNT	Holman, NWT	CHASME	70.7631	−117.8058	2000–2001
PINU	Pond Inlet, NU	CHASME	72.6970	−77.9750	2000–2001
SBNU	Taloyoak, NU	CHASME	69.5405	−93.5571	2000–2001
TULEG	Thule, Greenland	CHASME	76.4100	−68.5600	2000–2001
UPNG	Upernavik, Greenland	CHASME	72.7848	−56.1408	2000

Table 2. Events used in receiver function analysis for the CHASME seismic stations (each station recorded a subset of these events). Each event is identified by its origin time, in the format *yyjjjhhmmss,* where *y* denotes year; *j* Julian day; *h* hour; *m* minute and *s* seconds. Negative latitudes represent degrees south and negative longitudes represent degrees west. Event data come from the IRIS Data Management Centre.

Event	Latitude	Longitude	Depth (km)	Magnitude	Region
00217211302	48.786	142.246	10	7.1 MB	Sakhalin Island
00219072712	28.856	139.556	394	6.3 MB	Bonin Islands Region
00222114147	18.198	−102.480	45	6.1 MB	Michoacan, Mexico
00280043018	35.389	133.119	10	6.0 MB	Southern Honshu, Japan
00301042151	26.277	140.522	387	6.1 MB	Bonin Islands Region
00313065959	7.052	−77.885	17	6.0 MB	Panama–Colombia Border
00318155721	42.542	144.758	33	6.1 MB	Hokkaido, Japan
00334102514	−24.504	−70.549	58	5.8 MB	Near Coast of Northern Chile
00341171106	39.625	54.772	30	6.7 MB	Turkmenistan
00347052645	6.020	−82.682	10	5.8 MB	South of Panama
01013173330	13.063	−88.787	39	6.4 MB	El Salvador
01026031640	23.326	70.317	23	6.9 MB	India
01083062751	34.066	132.531	33	6.4 MB	Southern Honshu, Japan
01103153353	−59.663	−25.412	33	6.2 MB	South Sandwich Islands
01104232730	30.201	141.761	33	6.1 MB	South of Honshu, Japan
01116174857	43.230	145.750	82	5.9 MB	Hokkaido, Japan
01118044952	−18.028	−177.023	352	6.2 MB	Fiji Islands
01129154737	53.773	−164.249	40	5.7 MB	Unimak Island Region
01140042143	18.825	−104.299	33	5.5 MB	Jalisco, Mexico
01145004051	44.298	148.407	33	6.1 MB	Kuril Islands
01154024157	−29.811	−178.576	185	6.8 MB	Kermadec Islands
01164131755	24.484	122.400	78	5.7 MB	Taiwan Region
01165194847	51.207	−179.815	18	6.0 MB	Andreanof Islands, Aleutians
01174165108	55.103	−159.349	32	5.2 MB	Alaska Peninsula
01174203314	−16.224	−73.604	33	6.7 MB	Near Coast of Peru
01175131851	44.177	148.504	33	5.8 MB	Kuril Islands
01177041831	−17.739	−71.342	33	6.2 MB	Near Coast of Peru
01177140537	61.514	−140.007	10	5.8 MB	Southern Yukon Territory
01184131042	21.608	143.009	290	6.0 MB	Mariana Islands Region
01186135349	−15.562	−73.454	62	6.2 MB	Southern Peru
01188093843	−17.448	−72.041	33	6.6 MB	Near Coast of Peru
01200180040	57.250	−151.035	33	5.9 MB	Kodiak Island Region
01207002136	39.054	24.225	10	6.0 MB	Aegean Sea
01225201123	41.063	142.285	38	6.0 MB	Hokkaido, Japan Region
01285150216	12.662	144.917	37	6.7 MB	South of Mariana Islands
01318092610	35.945	90.535	10	6.1 MB	Qinghai Province, China
01332143226	15.471	−93.104	33	5.7 MB	Near Coast of Chiapas, Mexico
01336130153	39.438	141.088	124	6.1 MB	Honshu, Japan

While continental crust underlies most of the region shown in Fig. 1, the structure beneath a significant area of Baffin Bay has been found to be oceanic in nature. Thin crust, lineated magnetic anomalies and lineated gravity anomalies have been used (e.g. Jackson *et al.* 1979; Balkwill *et al.* 1990) to infer the presence of an extinct spreading centre formed by a rifting episode ∼60–40 Ma (e.g. Basham *et al.* 1977; Ziegler 1988). Oceanic crust also lies to the north of the Arctic archipelago.

1.1 Previous seismic studies

Information concerning the deep crustal structure of the Canadian Arctic archipelago is sparse, as few seismic studies of the region have been carried out. In the 1960s, several analyses of Rayleigh wave dispersion were carried out, modelling crustal thicknesses of 35–39 km across the region and into the Canadian Shield to the south (Brune & Dorman 1963; Buchbinder 1963; Wickens & Pec 1968; Wickens 1971). Simple continental crustal structures were inferred for the most part, the exception being the structure between Mould Bay and Coppermine in the western Arctic, where a layer of shear wave velocity 4.15 km s^{-1} at 35–50 km depth was required to match the dispersion curves (Wickens & Pec 1968). This velocity is higher than those typically associated with continental crust, but significantly lower than continental mantle shear wave velocities.

Crustal thicknesses of 34–42 km have been modelled for the Sverdrup Basin region, between Axel Heiberg Island to the east and Prince Patrick Island to the west, using seismic refraction profiling (Sander & Overton 1965; Overton 1970; Forsyth *et al.* 1979; Sobczak & Overton 1984). The crustal thicknesses include a sedimentary sequence, associated with the basin, of up to 15 km in thickness. Studies carried out to the north of the Arctic islands, across the continental margin, indicate crustal thicknesses of ∼22–30 km on the continental shelf edge (Berry & Barr 1971; Asudeh *et al.* 1989; Forsyth *et al.* 1994).

Geophysical studies carried out in Baffin Bay showed a significantly different local structure to that beneath the continental crust inferred for the Canadian Arctic archipelago and Greenland. Seismic refraction profiles (e.g. Keen *et al.* 1972) indicated much thinner crust of 10–12 km in central and northern Baffin Bay. Suppression of the L_g seismic phase along paths across the bay suggested that the thin crust was oceanic in nature (Wetmiller 1974).

A previous receiver function study carried out by Cassidy (1995) showed simple crustal structures with a sharp Moho in northeastern Canada. The Moho *P*-to-*S* conversion arrived later at station FRB (southern Baffin Island) than at more southerly seismic stations, indicating a thicker crust than that found in the southern Shield region. Cassidy (1995) also noted that receiver functions generated at the northern seismic stations RES and MBC were complex, '. . . [making] the continental Moho difficult to discern . . .'. This observation suggests a significant difference in crustal characteristics between the Shield regions and the Arctic archipelago.

2 DATA COLLECTION

The data set used in this study is a combination of broad-band teleseismic data from earthquakes recorded by 12 permanent and temporary seismic stations across the Canadian High Arctic (Fig. 1). Data are available from four permanent stations, of which three (FRB, RES and MBC) make up part of the Canadian National Seismograph Network (CNSN) and the fourth (ALE) is part of the network of seismic stations operated by the IRIS Data Management Centre.

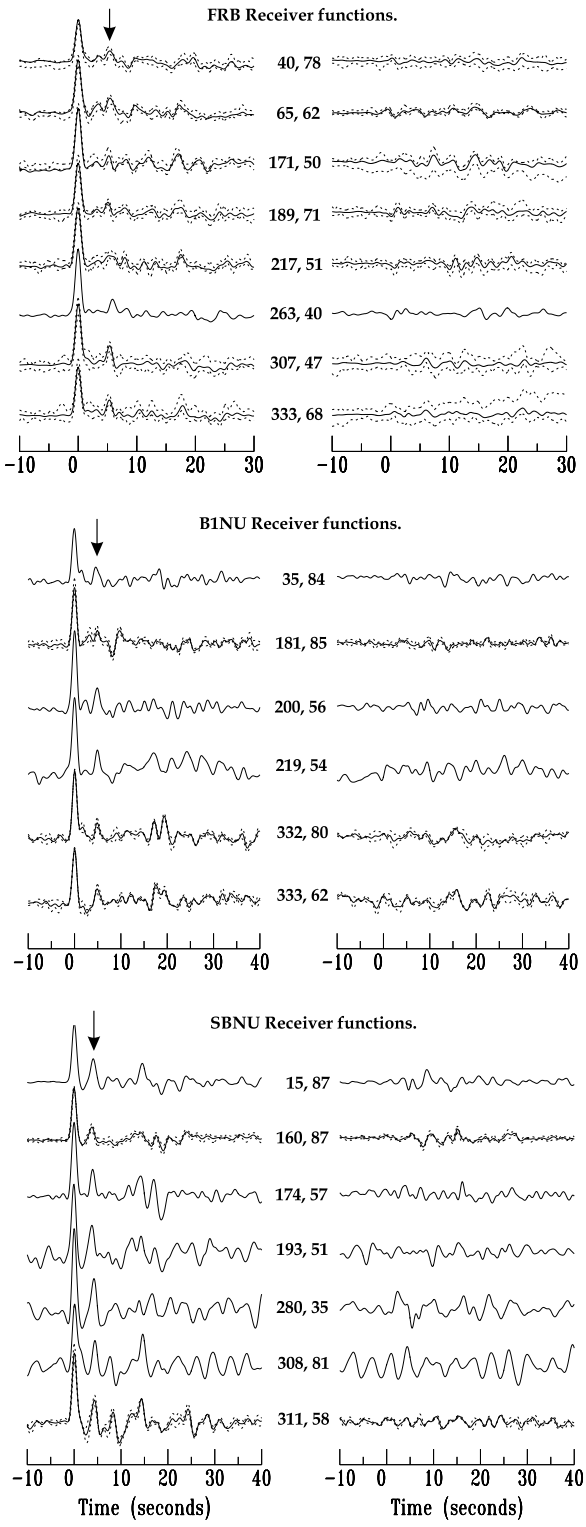

Figure 2. Receiver function data sets for stations FRB, B1NU and SBNU on the Canadian Shield. On this and subsequent similar figures, radial receiver functions are plotted on the left and tangential receiver functions are plotted on the right. All receiver functions are plotted to a common amplitude scale. The numbers in the centre of the plots are the backazimuth and epicentral distance, respectively, of the earthquake from the station. Single-event receiver functions are plotted as solid lines, and stacked receiver functions are plotted as solid lines surrounded by the $\pm 1\sigma$ stacking bounds (dotted lines). The vertical arrows at the top of each plot show the position of the Moho *P*-to-*S* conversion peak.

Of the three CNSN stations, FRB and RES are currently in operation, but MBC was closed down in mid-1997.

2.1 CHASME

The CHASME (Canadian High Arctic Seismic Monitoring Experiment) project was designed as a study of Earth structure and seismicity of northernmost Canada and the Baffin Bay region. During the summer and early autumn of 2000, seven three-component broad-band seismic stations were deployed across the Canadian High Arctic and western Greenland (Fig. 1, Table 1), at military and scientific bases and civilian communities. Nanometrics Orion digitizers, powered by mains electricity, record data from Guralp CMG-3ESP and CMG-40T broad-band sensors. The data are stored on 2 Gb hard discs, which are exchanged approximately once per month by local operators and sent to the Geological Survey of Canada in Ottawa. In addition, a set of data from two temporary seismic stations deployed on central Baffin Island by the Continental Geosciences Division of the Geological Survey of Canada was made available to the project (Snyder *et al.* 2002). These stations used Orion digitizers, powered by batteries, solar panel arrays and wind-powered generators, with Guralp CMG-40T broad-band sensors.

2.2 Earthquake data

This study uses *P* waveforms from large teleseismic earthquakes recorded by the stations. Earthquake bulletins were searched for events of magnitude 5.5 MB or greater, generally in the distance range 30°–90°, though a few nearer (some with magnitude <5.5 MB) and further (up to 155° away) events were also used. The waveforms for these events were extracted from the continuously recorded seismic data for each station. *P* waves with a high signal-to-noise ratio were selected from the set, for use in receiver function analysis. Data collection from the permanent CNSN and IRIS stations yielded a large number (several tens) of suitable events owing to the relatively long operation time of the stations. The largest number of receiver functions generated for one CNSN station was at station FRB, where the data set consisted of waveforms from 101 events. Subsets of the 38 events listed in Table 2 were used in the analysis for the temporary CHASME stations.

3 RECEIVER FUNCTION ANALYSIS

The shear wave velocity structure beneath each of the broad-band seismic stations is investigated using the method of receiver function analysis. The receiver function is the response of the structure beneath a seismograph site to an incident teleseismic *P* wave. At interfaces in the structure below the site, *P*-to-S_V conversions take place, so that the coda of the *P*-wave arrival at the site consists of a combination of *P* and S_V phases. Since the arrival angle of the seismic waves is steep, the vertical component seismogram is dominated by *P* waves and the radial component is dominated by the converted

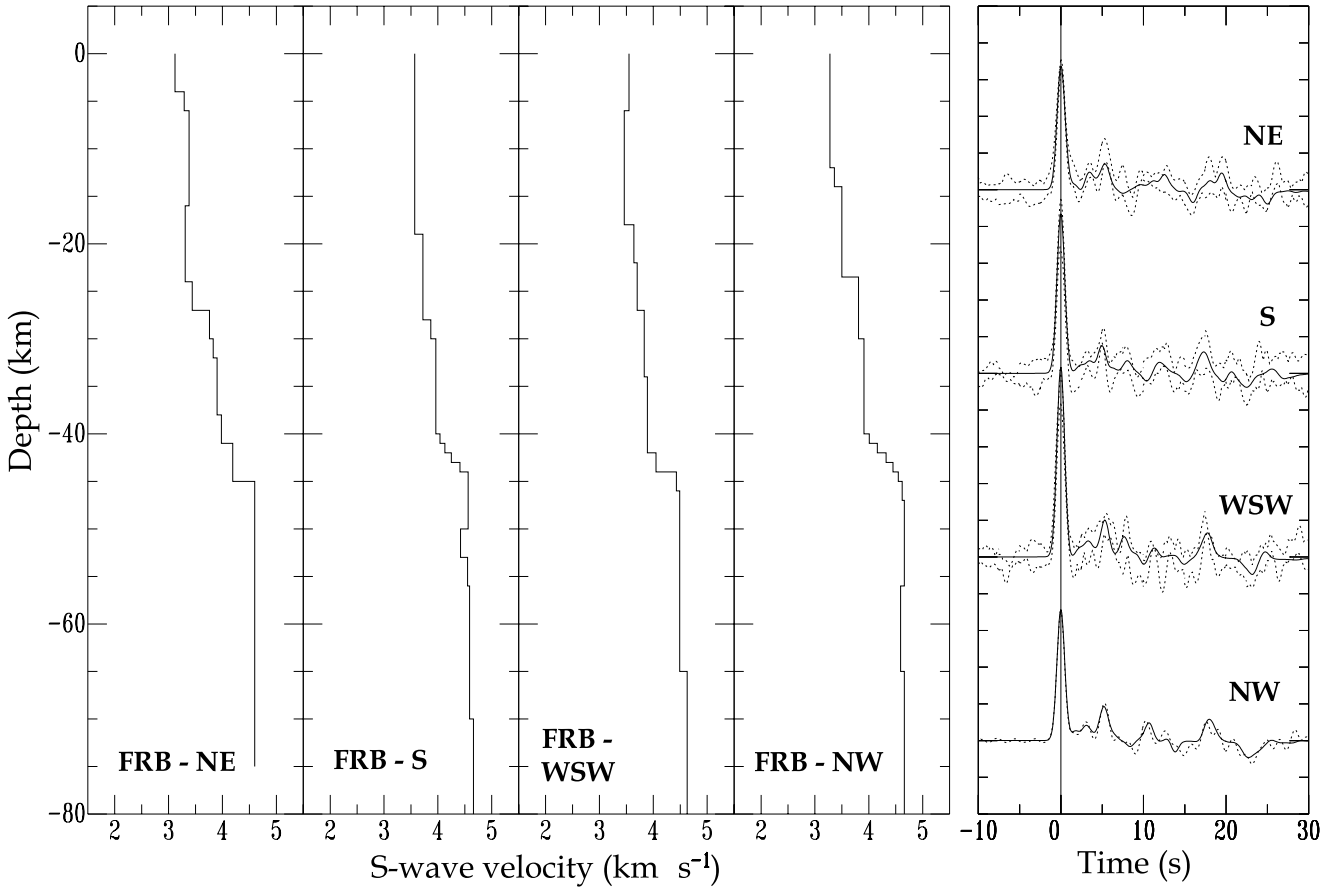

Figure 3. Crustal models and waveform fits for receiver functions from station FRB. Left-hand panels: velocity–depth models for different approach azimuths. Right-hand panel: corresponding waveform fits. Radial receiver function data are shown as dotted lines (a single line for a single-event receiver function; two dotted lines, representing upper and lower bounds, for a stacked receiver function) and synthetic radial receiver functions derived from the models are shown as solid lines.

S_V waves. In addition to the near-receiver response, the *P*-wave arrival and its coda contain information concerning the earthquake source function, near-source effects and deep mantle propagation effects. These are removed by deconvolving the vertical component seismogram from the radial and tangential component seismograms, and the resultant time-series is termed the 'receiver function'. True-amplitude receiver functions are formed using the deconvolution technique of Langston (1979) as modified by Ammon (1991). Stabilization of the receiver functions is achieved using the water-level method (Helmberger & Wiggins 1971; Clayton & Wiggins 1976) to fill spectral holes. The receiver functions are also smoothed by convolution with a Gaussian pulse. In this study, a Gaussian parameter of 1.5, which low-pass filters the waveforms at ∼0.7 Hz, is used, and water-level parameters in the range 0.0001–0.01 are used to fill spectral holes. The value of the water-level parameter is chosen individually for each receiver function, by inspection of the stability of the radial and tangential receiver functions, traded off against the form of the 'averaging function' (the deconvolution of the vertical component from itself; this waveform should resemble a narrow Gaussian pulse).

The receiver functions from different event backazimuths and epicentral distances are compared to assess the validity of a 1-D approximation to the structure beneath each seismic station. When the structure is 3-D, seismic energy is deflected away from the radial–vertical plane, giving rise to non-zero amplitudes on the tangential receiver functions. The amplitudes of the tangential receiver functions relative to those of the radial receiver functions give some indication of the degree of lateral heterogeneity beneath the seismic station, as does the variation in the details of the radial receiver function with backazimuth (e.g. Langston 1977; Cassidy 1992). Crustal anisotropy may also play a part in generating significant amplitudes on the tangential-component waveforms (e.g. Levin & Park 1998; Jones & Phinney 1998). Where the converted and reverberative phases in the radial receiver function are larger in amplitude than the tangential receiver functions, a 1-D approximation to the velocity structure is considered valid.

In cases where several receiver functions from similar event backazimuth and epicentral distance were available, the radial and tangential receiver functions were stacked to enhance signals and to suppress noise in the waveforms. For most of the Arctic seismic stations, the forms of the individual receiver functions suggest some degree of lateral heterogeneity in the crustal structure; therefore stacking bounds were mostly restricted to a maximum of ∼10° in backazimuth and epicentral distance (*cf.* Cassidy 1992). The long

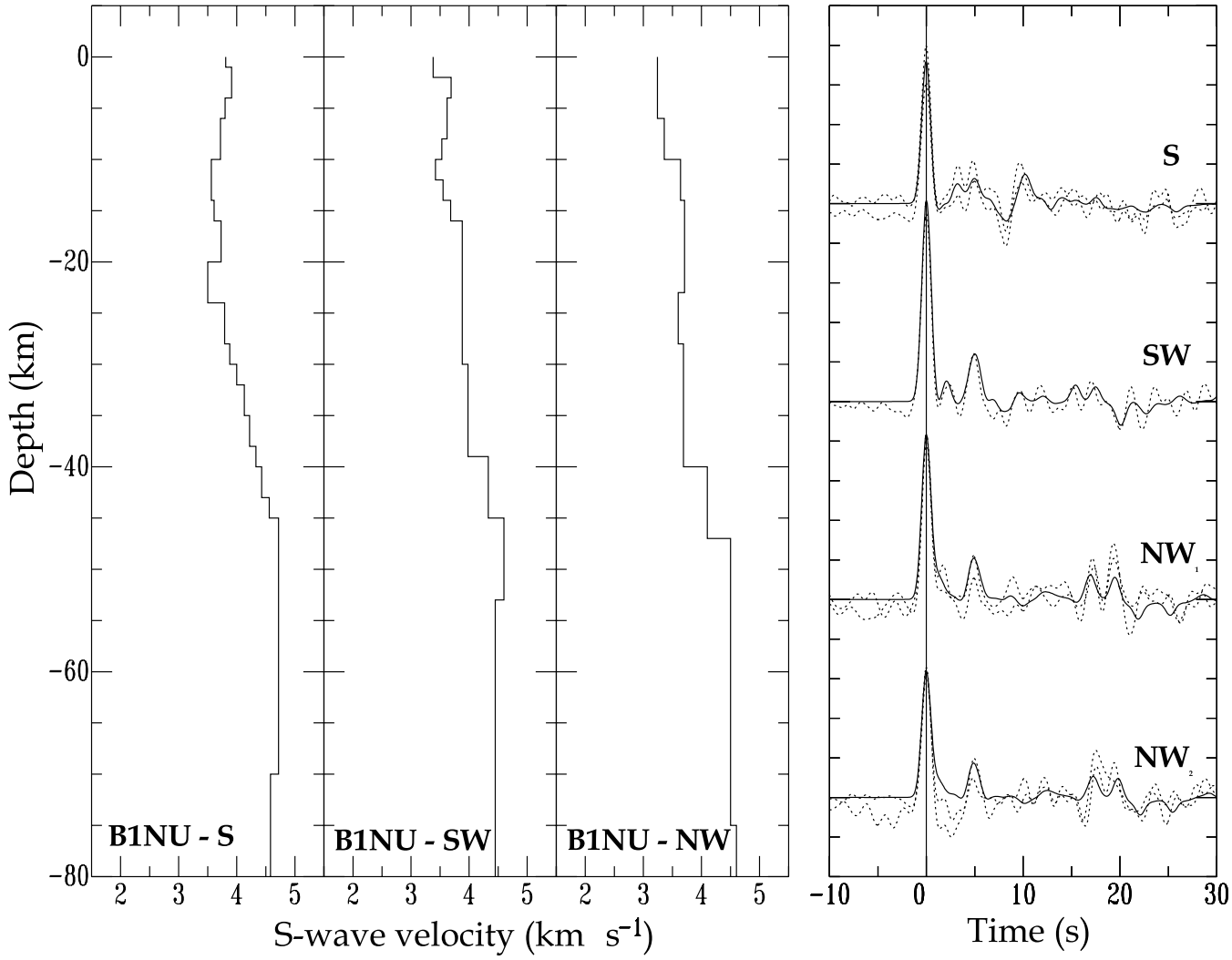

Figure 4. Crustal models and waveform fits for receiver functions from station B1NU. Refer to Fig. 3 for plotting conventions. Two northwest receiver functions are shown; these have similar backazimuth but different epicentral distances (80° and 62°).

recording duration of the CNSN stations allowed several receiver function stacks to be formed, some made up of 10 or more individual waveforms. In the case of the CHASME stations, the data sets are made up mainly of single-event receiver functions, with one or two stacked groups available.

The process that creates the radial and tangential receiver functions places the direct *P*-wave arrival '*Pp*' at 0 s in the radial time-series. An ideal *Pp* arrival is seen as a strong and fairly narrow peak in the time-series. However, where near-surface structure (such as low surface velocities overlying crystalline basement) exists beneath the seismic station, conversions and reverberations from near-surface discontinuities arrive soon after *Pp* (e.g. Cassidy 1995). The Gaussian function used to smooth and low-pass filter the receiver functions merges the signals, resulting in a single peak that is a combination of *Pp* with the arrivals associated with the near-surface structure. The peak is broadened compared with a pure *Pp* peak and is delayed slightly from zero time. This paper refers to the *apparent Pp arrival* when discussing this combined peak.

3.1 Modelling procedure

The shear wave velocity structure beneath each site was determined using a combination of inversion and forward modelling. The time-domain, linearized inversion procedure of Ammon *et al.* (1990) was used to obtain velocity models for the receiver functions from starting models that consisted of a stack of thin (1–5 km thick) horizontal layers, parametrized to a depth of 80–100 km. Where the receiver functions showed a clear Moho *P*-to-*S* conversion (e.g. stations FRB, SBNU), the depth to the Moho was estimated using simple one-, two- or three-layered models, and the crustal thickness thus obtained was used in the reference starting model. In some cases, some *a priori* information concerning crustal structure was available from previous studies (e.g. Wickens & Pec 1968; Buchbinder 1963), and this information was also incorporated into the starting models. Where no *a priori* information was available, and the depth to the Moho was not easily obtained from inspection of the receiver functions, a starting model based on the 'CANSD' model of Brune & Dorman (1963) was used.

In the inversion scheme of Ammon *et al.* (1990), shear wave velocity is the free parameter, while the layer thicknesses in the model remain fixed. The initial starting model is perturbed to give a set of new starting models, allowing the exploration of a wide initial model space and reducing the dependence of the solutions on the form of the initial model. In each case in this study, the radial receiver function was inverted from a set of 40 starting models. The difference between the radial receiver function and a synthetic waveform computed from each of the velocity–depth models is minimized, using a smoothness parameter that was chosen individually for each inversion set. In general, the method produces a range of solutions, clustered into 'families' of models. The variation in the forms of these model families arises from the trade-off between velocity and interface depth inherent in receiver function analysis.

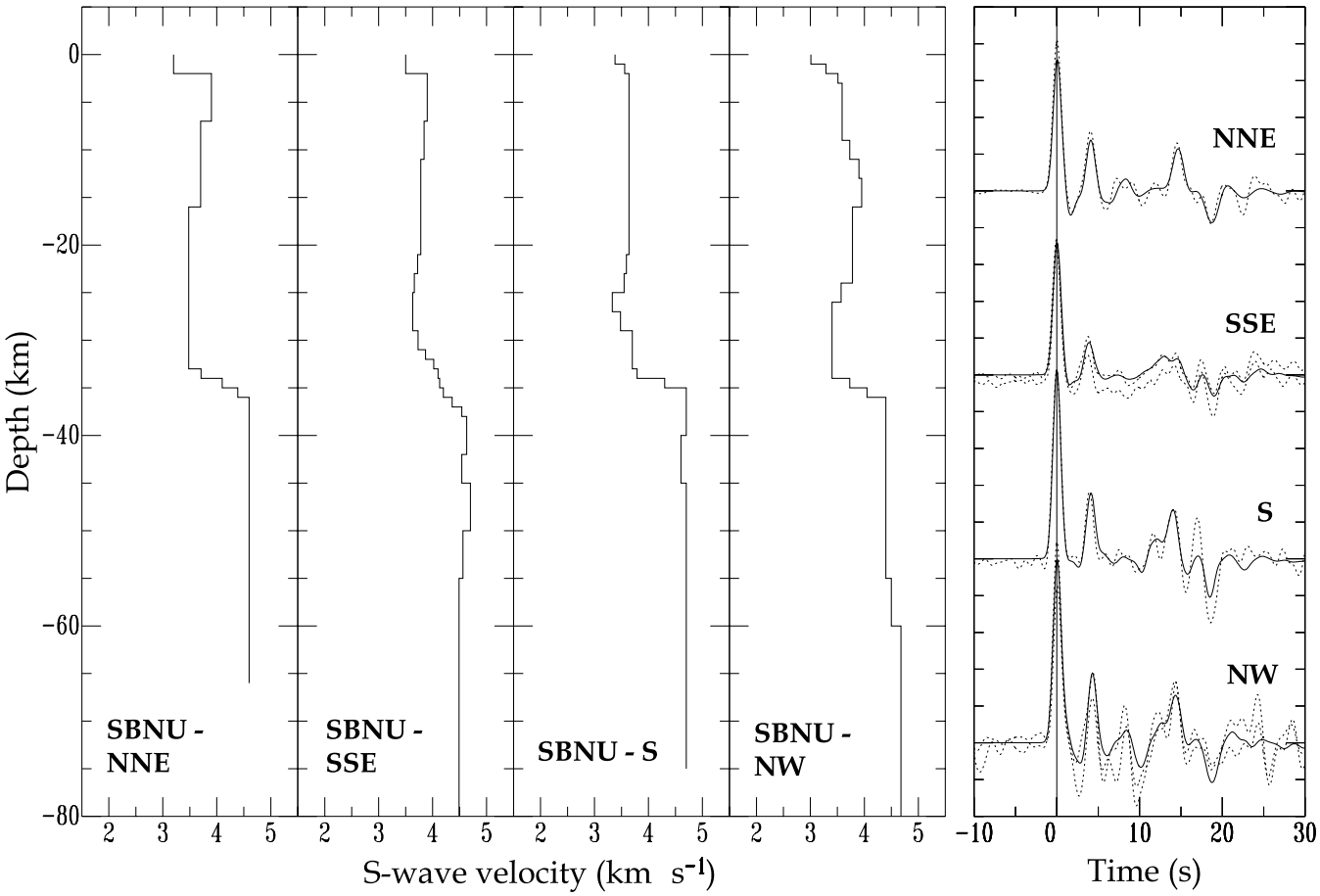

Figure 5. Crustal models and waveform fits for receiver functions from station SBNU. Refer to Fig. 3 for plotting conventions.

Geologically reasonable models that provided a good match to the data were selected for further study. In most cases, these models were simplified by merging layers of similar shear wave velocity, and then used as starting models in a second inversion with a narrower perturbation parameter. Representative models from the second inversion were then used as a basis for forward modelling.

Forward modelling was used to simplify the velocity–depth models further in order to match the main features of the radial receiver functions and to test the constraint of individual model features such as large discontinuities or low-velocity zones. The method of Randall (1989), using the reflection matrix formalism of Kennett (1983) was used to calculate synthetic seismograms for the simplified models, for which receiver functions were calculated using the same method as that employed for the original data.

In general, individual inversion and forward models were developed for several different receiver functions at each site, giving 1-D approximations to structure at different azimuths from the station. This method allows some constraint on lateral structural variation, resulting in a pseudo-3-D interpretation of the crustal structure beneath each seismic station. Two exceptions to this modelling procedure were made, at Mould Bay (station MBC) and Holman (station HMNT). Both of these stations show a strong degree of lateral heterogeneity, manifested by large-amplitude tangential receiver functions with distinct patterns of polarity reversals. However, most of the strong arrivals in the radial receiver functions are well-correlated across all azimuths. Following the examples of Cassidy (1995) and Zelt & Ellis (1999), a 1-D approximation to the structure beneath MBC and HMNT was developed by inverting and forward-modelling receiver functions from a set of all-azimuth stacks (grouped according to the epicentral distance), which suppress the features arising from 3-D structure and enhance those arising from near-horizontal planar interfaces.

A further set of forward models was developed at station MBC, where the variation in the tangential receiver functions with event backazimuth strongly suggested the presence of a dipping layer within the crustal section. Here, a dipping layer was placed into the 1-D velocity–depth model and synthetic radial and tangential waveforms were calculated for a range of backazimuths, using the *ray3d* program of Owens, based on the method of Langston (1977). Trial values of interface strike and dip were modelled until a satisfactory fit could be found to the pattern of arrivals in the tangential receiver function data.

The principal aim of the forward modelling stage is to produce the simplest possible velocity–depth model that provides an adequate fit to the important features in the receiver function waveforms. In some cases, especially where the receiver function data are noisy, or contain features that are likely to be associated with scattering from laterally heterogeneous structure, it is undesirable to seek a perfect fit to every arrival in the waveform. Forward modelling, where the analyst can assess the importance of the features in the velocity–depth models, is therefore essential in order to obtain meaningful results. The simplified forward models generally contain the principal features of the inversion models, but with a significantly reduced number of parameters. When the final model has been obtained, further forward modelling is used to test the significance of specific features such as low-velocity zones, low near-surface velocities and the sharpness of the Moho.

The resolution of the models derived from the receiver function analysis is dependent on the frequency of the waveforms (e.g. Sheriff & Geldart 1982). The vertical resolution is approximately one-quarter of the shortest wavelength; for receiver functions low-pass filtered at 0.7 Hz, this corresponds to a minimum resolvable layer thickness of ∼2 km. The lateral sampling of the receiver function for a given interface is taken as the radius of the first Fresnel zone of the incoming *P* wave:

$$R = \sqrt{(z + \lambda/2)^2 - z^2}, \tag{1}$$

where z is the depth of the interface, λ is the wavelength of the incident *P* wave and *R* is the radius of the Fresnel zone. For a crustal thickness of 35 km, the lateral sampling radius at the Moho would be ∼15 km.

Throughout the models, the Poisson ratio is kept fixed at a value of 0.25. The density of the layers is calculated from the *P*-wave velocity, using the relationship $\rho = 0.32\ V_p + 0.77$ (Berteussen 1977).

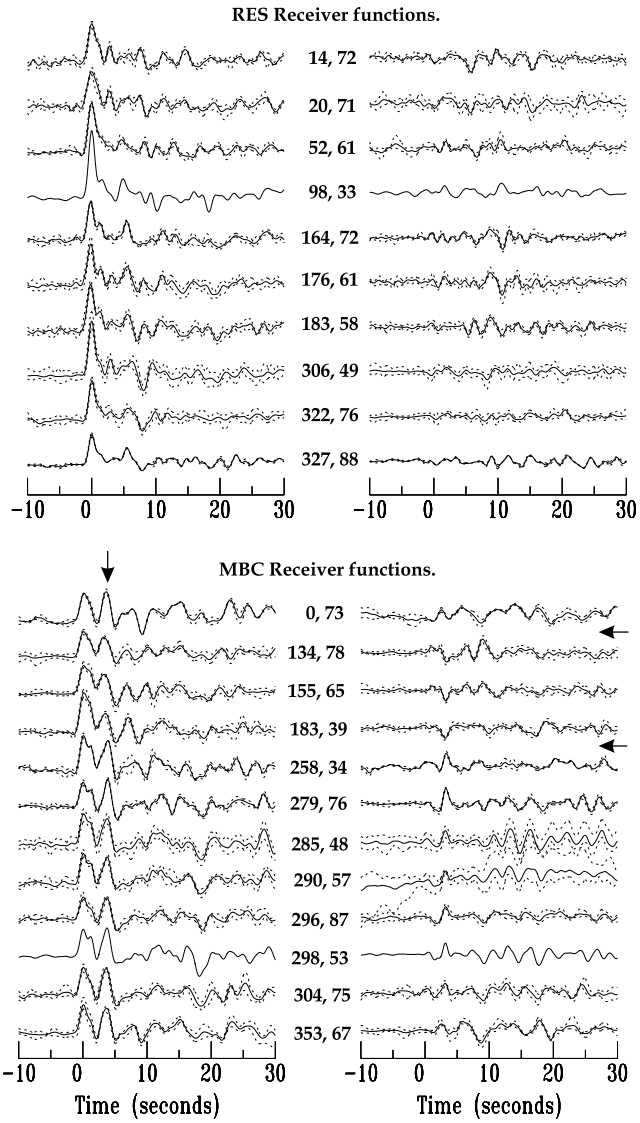

Figure 6. Receiver function data sets for stations RES and MBC in the northern/western Arctic archipelago. Plotting conventions as for Fig. 2. For station MBC, the vertical arrow indicates a peak that is a combination of reverberations from an interface at 5 km depth with the Moho *P*-to-*S* conversion. The horizontal arrows between successive tangential receiver functions indicate polarity reversals.

4 RECEIVER FUNCTION MODELS ACROSS THE ARCTIC REGION

4.1 Canadian Shield

Three stations lie on Canadian Shield rocks; two (FRB, B1NU) on southern Baffin Island and one (SBNU) on the Boothia Peninsula. Fig. 2 shows the receiver function data sets for the three Shield stations.

4.1.1 Iqaluit; station FRB

Some azimuthal variation exists in the radial and tangential waveforms at station FRB, but a peak at ∼5 s after the direct *P*-wave arrival is visible at all azimuths, strongest in the receiver functions from northwestern approaches. The 5 s peak is interpreted as the *P*-to-*S* conversion at the Moho, and patterns of peaks and troughs at 15–25 s after *Pp* are consistent with Moho reverberations. Preliminary forward modelling of one of the northwestern waveforms suggests a relatively simple crustal structure, with a prominent Moho at ∼45 km and at least one velocity discontinuity within the crust. There is no evidence in the receiver functions for a low-velocity surface layer beneath the station, consistent with the site position on crystalline basement rocks.

Inversion and forward modelling of the receiver function stacks with the highest signal-to-noise ratios (Fig. 3) shows that layering within the crustal section is necessary in order to match the peaks and troughs in the radial waveforms at 1–4 and 6–15 s. Some waveforms are best matched by additional structure below the Moho, but this structure is not well-constrained. The nature of the Moho itself varies between different azimuths; a sharp discontinuity is required to match the data for certain azimuths while, at others, a more gradational transition is more appropriate. In all cases, the Moho is required to be a prominent feature in order to match the strong signals in the radial receiver functions. The Moho depth beneath FRB is 44 ± 2 km.

4.1.2 Central Baffin Island; station B1NU

Station B1NU, operated by the Continental Geoscience Division of the Geological Survey of Canada, has a total of 19 receiver functions from almost a 1 yr recording period. A peak at ∼5 s,

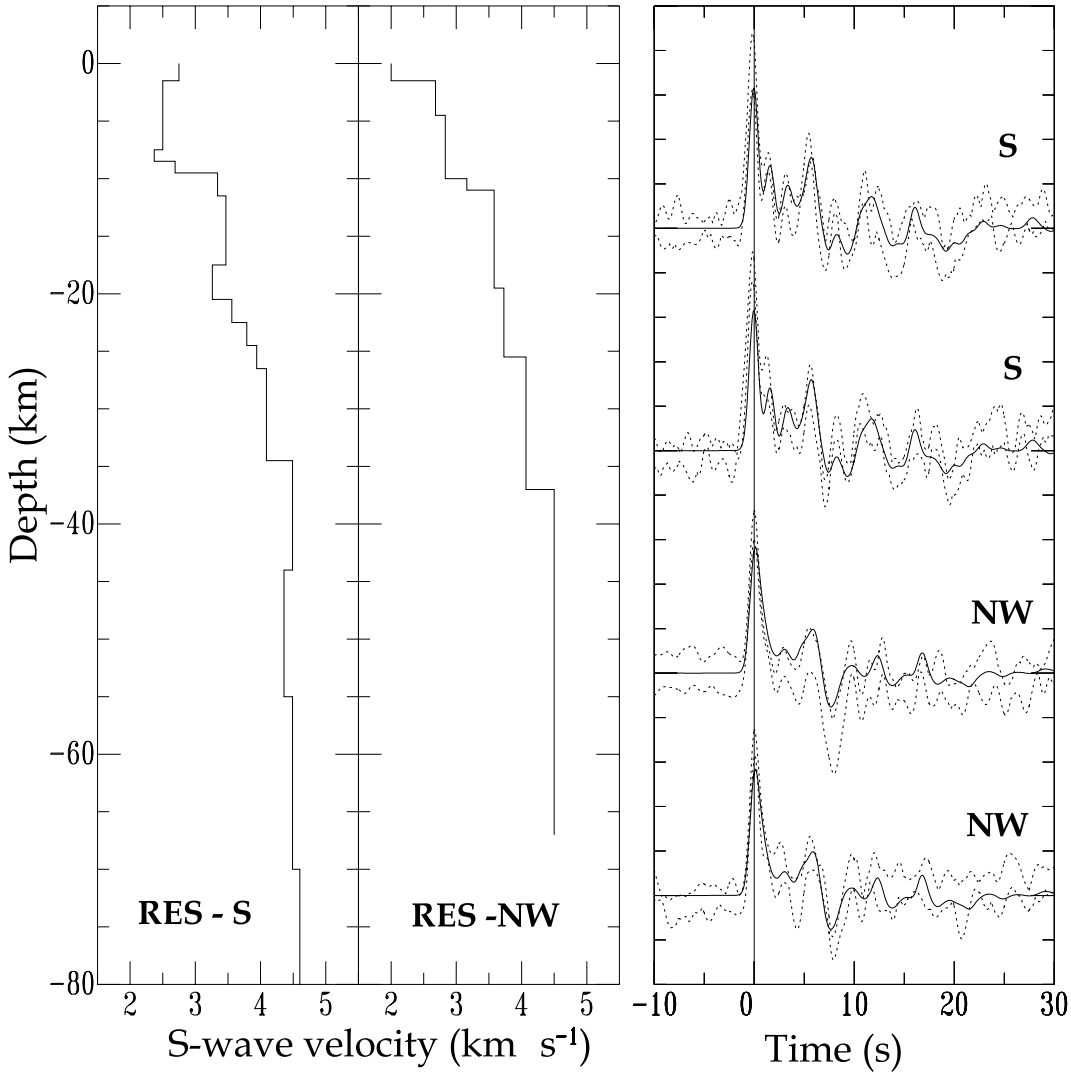

Figure 7. Crustal models and waveform fits for receiver functions from station RES. Refer to Fig. 3 for plotting conventions. The two receiver functions from each direction have similar backazimuth but different epicentral distances (61° and 58° for southern receiver functions; 49° and 76° for northwestern receiver functions).

probably representing the Moho *P*-to-*S* conversion, is seen at all azimuths, though its amplitude relative to other features in the waveform varies with event backazimuth. The peak is strong for events approaching from the north, southwest and northwest, but weaker for events approaching from due south. In addition, prominent features in the northwestern receiver functions at ∼15–25 s may represent reverberations associated with the Moho. Structure in the first 5 s of the waveform suggests layering within the crust.

For events approaching from the northwest, the waveforms can be fitted by a relatively simple model (Fig. 4) with some crustal layering and a low-velocity zone at ∼25 km depth. In order to match the doubled peaks at 17–20 s, a crust–mantle transition consisting of two sharp discontinuities is required. A similar feature is used to match the waveform from a southwestern event, though the double peaks are not such strong features in this case as for the northwestern events. The mid-crustal low-velocity zone is required to match features in the waveforms between 8 and 16 s.

The stack of receiver functions from events approaching from the south has a less prominent peak at 5 s and little energy at 15–25 s; the strongest feature in the waveform is a negative arrival at 9 s followed by a positive arrival at 11 s. The best waveform fit is achieved by a model with predominantly gradational velocity changes within the crustal section (Fig. 4), except for a prominent low-velocity zone at 20–25 km depth. *P*-to-*S* conversions from the interfaces at the top and base of the low-velocity zone are required to match the waveform at ∼3 s, and the arrivals at 8–12 s are matched by the corresponding reverberations.

For all azimuths, the transition from crustal velocities to mantle velocities occurs over a depth range of ∼39–46 km.

4.1.3 Taloyoak (Spence Bay); station SBNU

The Taloyoak data set shows the simplest set of receiver functions of the stations in the CHASME temporary seismic array. Some azimuthal variation in the waveforms exists, with more complex receiver functions for the northwestern-approaching events than the northeastern, southeastern and southern events. A very prominent peak at ∼4 s probably represents the *P*-to-*S* conversion at the Moho, and the reverberations from this interface are also seen in the receiver functions, between 14 and 24 s after the direct *P*-wave arrival.

Inversion and forward modelling (Fig. 5) yields a set of fairly simple models in which the most prominent feature at each azimuth is the Moho, at a depth of 35–36 km. Some structure within the crust, such as low-velocity zones in the 20–30 km depth range, is needed to match the features of the waveforms between ∼5 and 13 s. The doubled negative arrival at 15–20 s in the southern receiver functions is matched by the inclusion of a low-velocity zone in the mantle, ∼5 km beneath the Moho.

4.2 Sverdrup Basin margins

Station RES lies just south of the southern margin of the Sverdrup Basin, within the Cornwallis Fold Belt complex. Station MBC lies at the westernmost point of the Basin, at its border with the Franklinian

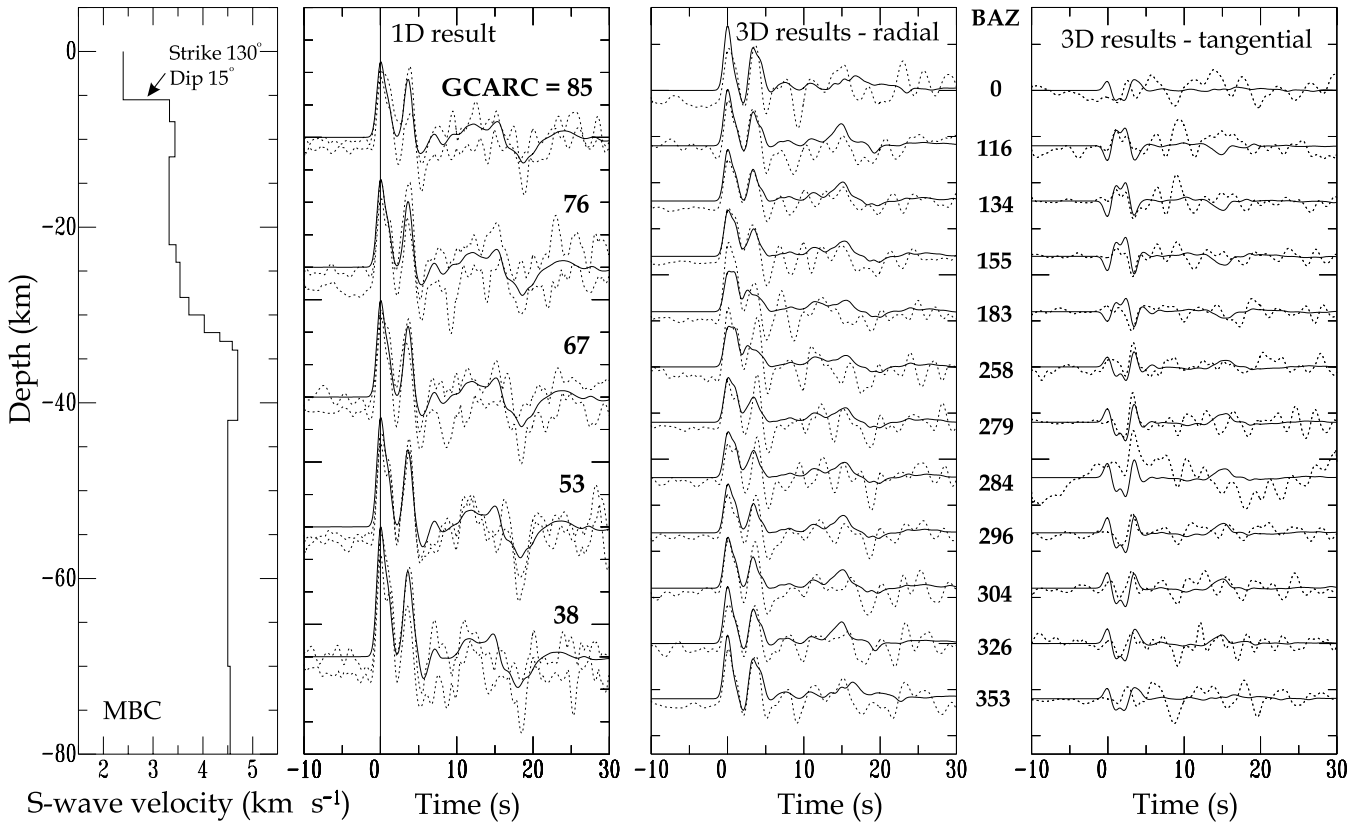

Figure 8. Crustal models and waveform fits for receiver functions from station MBC. From left to right: velocity–depth model with dipping interface; fits of synthetic radial receiver functions (solid lines) to all-azimuth stacked radial data (dotted lines; lower and upper stacking bounds) at different epicentral distances ('GCARC'), using a 1-D modelling procedure; 3-D modelling results (solid lines) for radial and tangential receiver function data (dotted lines) over a range of backazimuths from 0° to 353°.

province to the southwest and the Arctic Coastal Plain to the north. Receiver functions for the two stations are shown in Fig. 6.

4.2.1 Resolute; station RES

Relatively large tangential amplitudes and considerable variation in the radial receiver functions with backazimuth indicate that the crust beneath station RES has a high degree of lateral heterogeneity. Inspection of the radial receiver function stacks shows three main clusters of waveform type, in the north, south and northwestern approaches. Each of these clusters has a significantly different waveform to the others, therefore a different crustal model has been developed for each azimuth group (Fig. 7).

The northern receiver functions are modelled (not shown in Fig. 7) with a relatively simple layered crust, a sharp Moho at 35 km depth and two low-velocity zones. The amplitudes of the receiver functions are not well matched because of the poor quality of the receiver function data, but the major features of the structure can nevertheless be resolved.

Layered models are also used to match the features of the southern and northwestern receiver functions. The details of the models differ; in particular, the southern receiver functions require a more complex model, including two crustal low-velocity zones, to match the data. However, two features are common to both models, a large increase in velocity at ∼10 km depth and a sharp Moho. The Moho depth is 34 km in the southern model and 37 km in the northwestern model.

4.2.2 Mould Bay; station MBC

The MBC radial receiver functions are dominated by a very large amplitude arrival approximately 3.5 s after the direct *P* arrival. The apparent *Pp* peak generally shows a shoulder at 1 s, and the 3.5 s arrival matches the apparent *Pp* peak in amplitude at most azimuths. No other strong features are apparent in the waveforms, though later arrivals correlate well across all azimuths. The highest-quality tangential receiver functions have a distinct arrival at ∼3 s, the polarity of which reverses twice over the 360° backazimuth range, once in the northeast and once in the southwest, suggesting the presence of dipping structure beneath the station. Simple forward modelling suggests that the large-amplitude arrivals in the radial waveform can be explained by the presence of a low-velocity surface layer several kilometres thick, at the base of which is a large velocity discontinuity. The combination of reverberation from this interface and conversion at the Moho gives rise to the large peak at 3.5 s.

The structure beneath MBC is modelled using a set of five all-azimuth stacks grouped according to event epicentral distance (*cf.* Zelt & Ellis 1999). The main features of the waveforms can be fitted with a fairly simple model (Fig. 8). A 5 km thick low-velocity surface layer overlies a nearly uniform crustal section. The Moho is a gradational feature, with the best-fitting models showing a crustal thickness of approximately 33 km. A lid structure at 34–42 km depth provides a further improvement to the waveform fit.

3-D forward modelling was carried out to investigate the effect of a dipping interface in the crustal section. The pattern of polarity reversals in the MBC tangential receiver functions suggests that the updip/downdip directions of a dipping interface, where the tangential receiver function would have zero amplitude (e.g. Cassidy 1992), lie in the backazimuth ranges 0°–116°/183°–258°. 3-D forward modelling for a range of strikes from 120° to 180° gives the best waveform fits to the radial and tangential

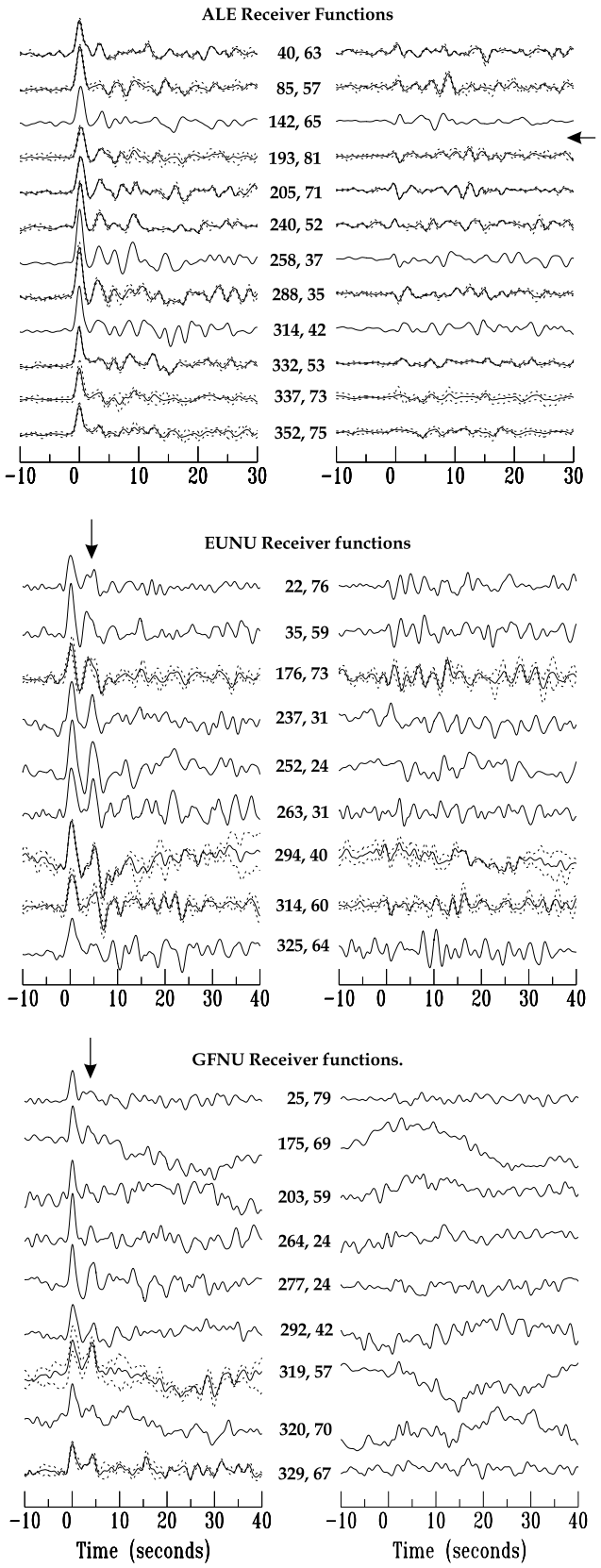

Figure 9. Receiver function data sets for stations ALE, EUNU and GFNU on Ellesmere Island. Plotting conventions as for Fig. 2. The vertical arrows at the top of the EUNU and GFNU plots show the position of the Moho *P*-to-*S* conversion peak, and the horizontal arrow within the ALE tangential receiver functions indicates a polarity reversal.

receiver functions when the base of the low-velocity surface layer dips to the southwest at 15°, with a strike of 130°. A dipping-layer model provides a good match to the pattern of polarity reversals in the tangential receiver functions, though crustal anisotropy might be a possible alternative explanation for the observations.

4.3 Ellesmere Island

The three Ellesmere Island stations lie within different geological provinces of the High Arctic. ALE lies on Franklinian structures, EUNU lies within the Sverdrup Basin region and GFNU lies on the border of Canadian Shield material with the Franklinian province. Receiver function data sets are shown in Fig. 9.

4.3.1 Alert; station ALE

Like Resolute, the structure beneath Alert appears to contain a strong degree of lateral heterogeneity, shown by azimuthal variation in the radial receiver functions and significant amplitudes in the tangential receiver functions. There is some evidence for the presence of dipping structure (though crustal anisotropy may also be a factor), with a polarity reversal at zero time in the tangential receiver functions between 142° and 193°, but the pattern of arrivals in the tangential receiver functions is not sufficiently clear to carry out dipping-layer 3-D receiver function modelling. Instead, 1-D crustal models are developed for different azimuths to give information on the structural variations with azimuth beneath the seismic station (Fig. 10). The details of the models vary considerably, but the depth at which shear wave velocities reach values typically associated with the mantle are fairly consistent, lying in the range 26–32 km. In most cases, structural variations in both the crust and the uppermost mantle are required to give a reasonable match to the arrivals in the radial receiver functions. Several models contain low-velocity zones, though whether these features are genuine LVZs or artefacts of heterogeneous structure cannot be resolved, owing to the lack of consistency in LVZ depth and thickness over different event backazimuths.

4.3.2 Eureka; station EUNU

Significant amplitudes in the tangential receiver function set and azimuthal variations in the radial receiver functions indicate a laterally heterogeneous structure beneath Eureka. The most prominent feature in the radial waveforms is a large, broad peak at ∼4–6 s. The apparent *Pp* arrival is shifted from zero time and is, at several azimuths, followed by a negative arrival. The features of the waveforms between 0 and 7 s suggest that near-surface velocities are low compared with the crust as a whole. Several positive and negative arrivals between 5 and 15 s in the radial receiver functions suggest structure within the crust and in the uppermost mantle.

The forward models for the Eureka receiver functions from the south, west and northwest (Fig. 11) all require low near-surface velocities (∼1.5–1.8 km s^{-1}) in order to match the data, suggesting the presence of a few kilometres of sediments beneath the station. The models also feature crustal layering, including low-velocity

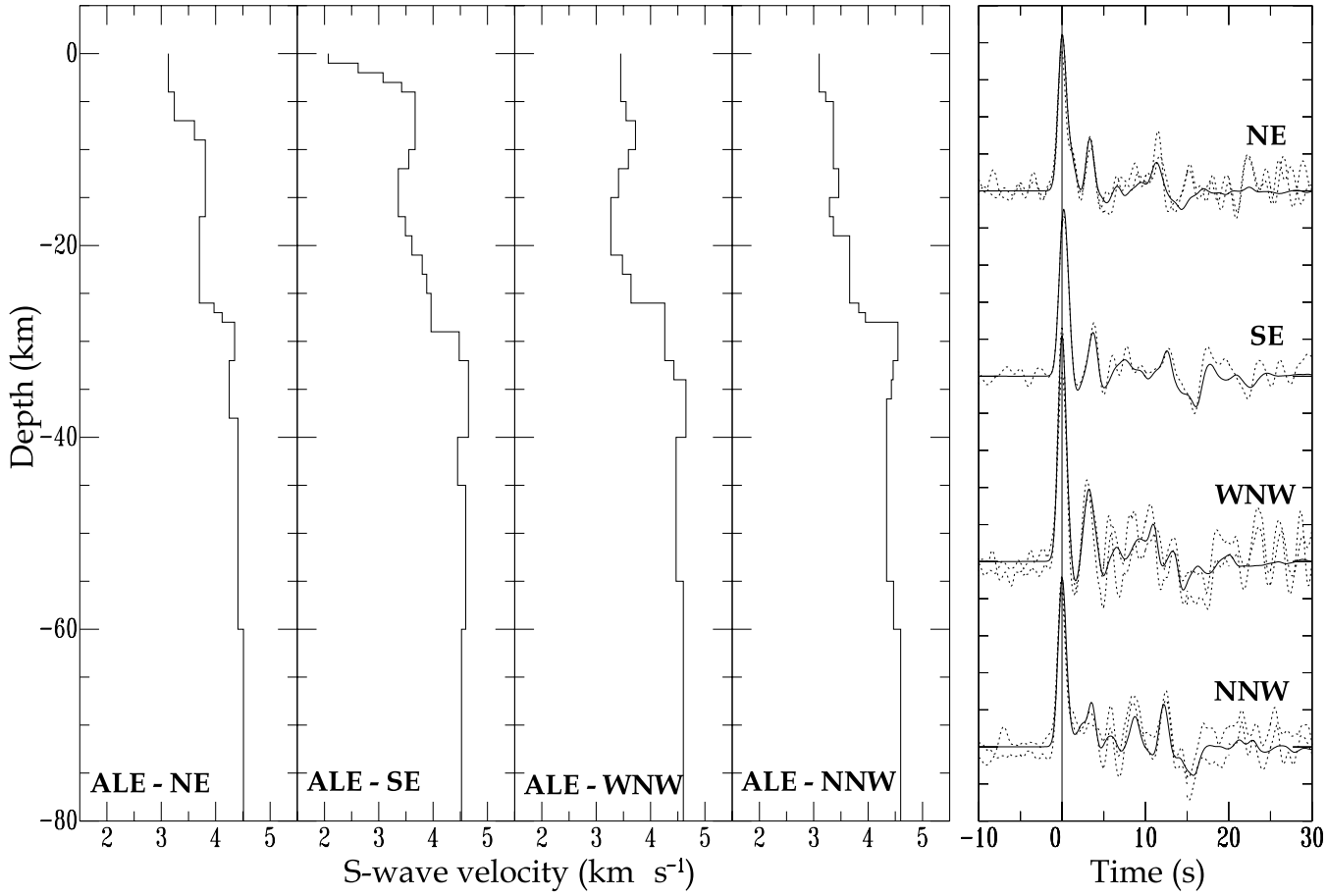

Figure 10. Crustal models and waveform fits for receiver functions from station ALE. Refer to Fig. 3 for plotting conventions.

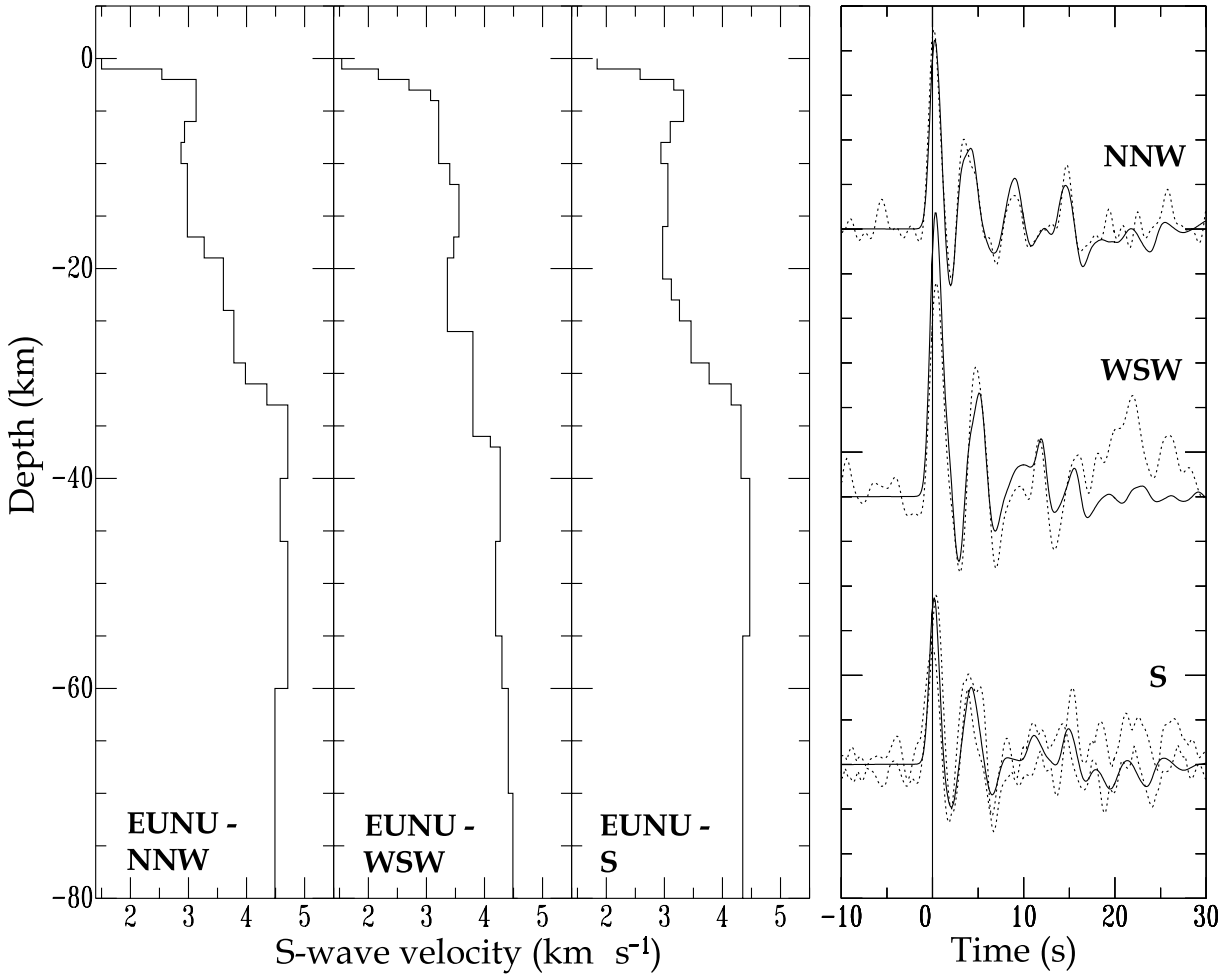

Figure 11. Crustal models and waveform fits for receiver functions from station EUNU. Refer to Fig. 3 for plotting conventions.

zones. The Moho is a gradational feature at a depth of 33–36 km, and some layering within the mantle is required to match the waveforms.

4.3.3 Grise Fiord; station GFNU

Most of the GFNU receiver functions are noisy, and many show instability related to the deconvolution process, with long-period signals superimposed on the waveforms. However, at most azimuths, a peak at ∼4 s is observed, which is strongest in the western receiver functions. This peak most probably represents the *P*-to-*S* conversion at the Moho. The corresponding signals from Moho reverberations are generally not visible, though a peak at ∼16 s in the northwesternmost receiver function set may represent a reverberation.

The best fit to receiver functions from Japanese events (the northwesternmost backazimuth) is obtained from a model where the *S*-wave velocity increases gradationally in the upper and mid-crust, with a thick constant-velocity layer deeper in the crust (Fig. 12). The Moho is a prominent discontinuity at 34 km, with some deeper structure required to achieve a good match to the waveform between 15 and 22 s. The noisier southern receiver functions are fitted with a simple model (not shown); a thin low-velocity section overlies a constant-velocity crust with a prominent discontinuity at 29 km depth and a transition to mantle-type velocities between 29 and 36 km depth.

4.4 Western Arctic—Holman; station HMNT

Of the temporary seismic stations analysed in this study, Holman has the largest set (25 events) of high-quality receiver functions, with a good azimuthal coverage everywhere except the northeastern quadrant (Fig. 13). The radial receiver functions are characterized by a set of prominent positive and negative arrivals that correlate well across all azimuths. It is not obvious which, if any, of these arrivals represents a Moho *P*-to-*S* conversion. Tangential receiver functions at Holman are mostly of large amplitude, sometimes larger than the arrivals (apart from the apparent *Pp* arrival) on the corresponding radial receiver functions. The polarity of the first arrival (at zero time) changes with event backazimuth, with at least three reversals over 360°. This suggests not only that the structure below Holman is 3-D, but also that it is more complex than could be accounted for by a simple dipping-layer model, in which the polarity of the tangential signal would reverse only twice over a 360° range (e.g. Cassidy 1992). A pattern of more than two polarity reversals over 360° probably indicates anisotropy within the lithosphere beneath the station (e.g. Jones & Phinney 1998).

A full 3-D treatment of the Holman receiver functions is beyond the scope of this paper. Instead, a 1-D approximation to the crustal structure is sought, using the fact that most of the strong arrivals in the radial receiver functions correlate well across all azimuths. Following the example of Zelt & Ellis (1999), all-azimuth stacks were made for the Holman receiver functions for average epicentral

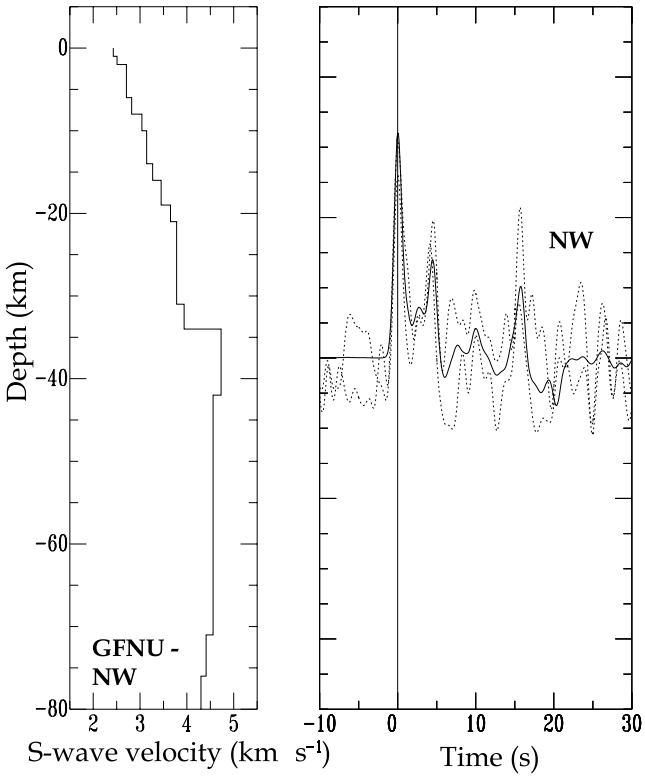

Figure 12. Crustal models and waveform fits for receiver functions from station GFNU. Refer to Fig. 3 for plotting conventions.

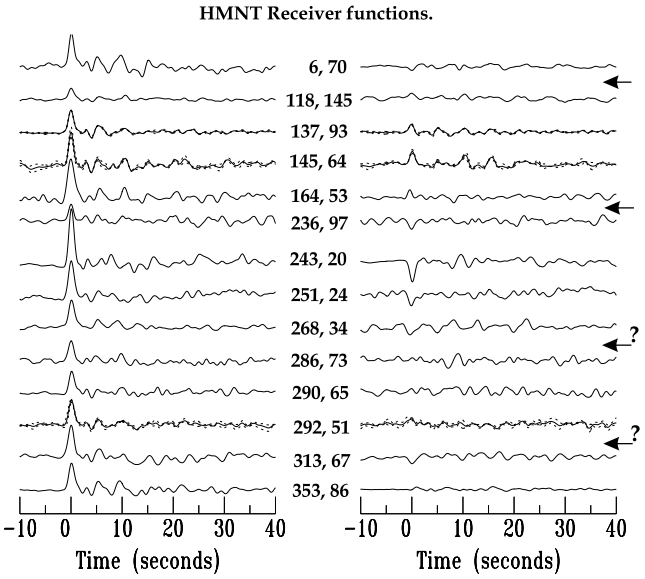

Figure 13. Receiver function data set for station HMNT in the western Arctic. Plotting conventions as for Fig. 2. Horizontal arrows between successive tangential receiver functions indicate polarity reversals.

distances of 92°, 69° and 55°, and a 1-D model was obtained using the same method as that used for the other receiver function models described in this paper (Fig. 14).

The best-fitting model consists of a series of layers, with two low-velocity zones within the top 20 km of the model. No obvious Moho exists; velocities are similar to those associated with the continental lower crust down to a depth of 35 km, but velocities typically associated with the mantle are not reached until a depth of 55 km. From 35 to 55 km, *S*-wave velocities increase gradually from 4.0 to 4.3 km s^{-1}.

4.5 Baffin Bay coastlines

Unlike central Baffin Bay, the coastlines bordering the bay lie on Shield material. The Canadian side of the region is very seismically active (e.g. Basham *et al.* 1977); the Greenland coast appears to be more stable.

4.5.1 Pond Inlet; station PINU

At Pond Inlet on the northeast coast of Baffin Island, receiver functions were generated for several large teleseismic events, but all were considered to be of insufficient quality for detailed inversion and forward modelling, owing to high levels of noise and ringing in the waveforms. One peak correlates well across all azimuths; this peak arrives at 3.5–4 s after the apparent *Pp* arrival. Assuming that this peak represents the *P*-to-*S* conversion at the Moho, simple forward modelling, using shear wave velocities comparable to those modelled at other Arctic seismic stations, suggests a crustal thickness of ∼35 km.

4.5.2 Thule, Greenland; station TULEG

The receiver functions generated from events recorded at TULEG (Fig. 15) tend to be noisy, with long-period signals superimposed on some of the waveforms, and ringing in several of the radial receiver functions. Azimuthal variations in the radial receiver functions indicate laterally heterogeneous structure. At ∼3–5 s, a broadened or doubled peak is visible in most of the radial receiver functions, with the 5 s portion of the arrival strong in the northwestern waveforms.

Structure within the crust is needed to fit the southern receiver function (Fig. 16), but the azimuthal variation in the radial and tangential receiver functions suggest that some of this apparent structure may be an artefact of scattering from laterally heterogeneous structures. In order to match the delay in the apparent *Pp* arrival, and to fit the first negative arrival, a low-velocity surface layer is required. The transition to velocities typically associated with the mantle occurs over a depth range of 35–40 km.

The northwestern model, like the southern model, requires low velocities (∼2 km s^{-1}) at the surface in order to match the offset of the apparent *Pp* arrival from zero, and to match the subsequent negative arrival. A relatively simple model is used to match the main features of the receiver function; more detail would be inappropriate owing to the noise levels and long-period signal in the data. Some layering is present within the crust, and the broadened peak at 13–17 s is matched by steps in velocity above the Moho, which lies at 37 km depth.

4.5.3 Upernavik, Greenland; station UPNG

Insufficient data were available at Upernavik to enable detailed receiver function modelling, owing to a short recording period. Receiver functions generated with a Gaussian value of $a = 1.5$ were subject to ringing, but longer-period receiver functions ($a = 1.0$) gave more stable waveforms, though these were still too noisy to justify detailed modelling. All of the longer-period receiver functions show a prominent peak at 4.1 s after the apparent *Pp* arrival. Assuming this peak to be the *P*-to-*S* conversion at the Moho, a

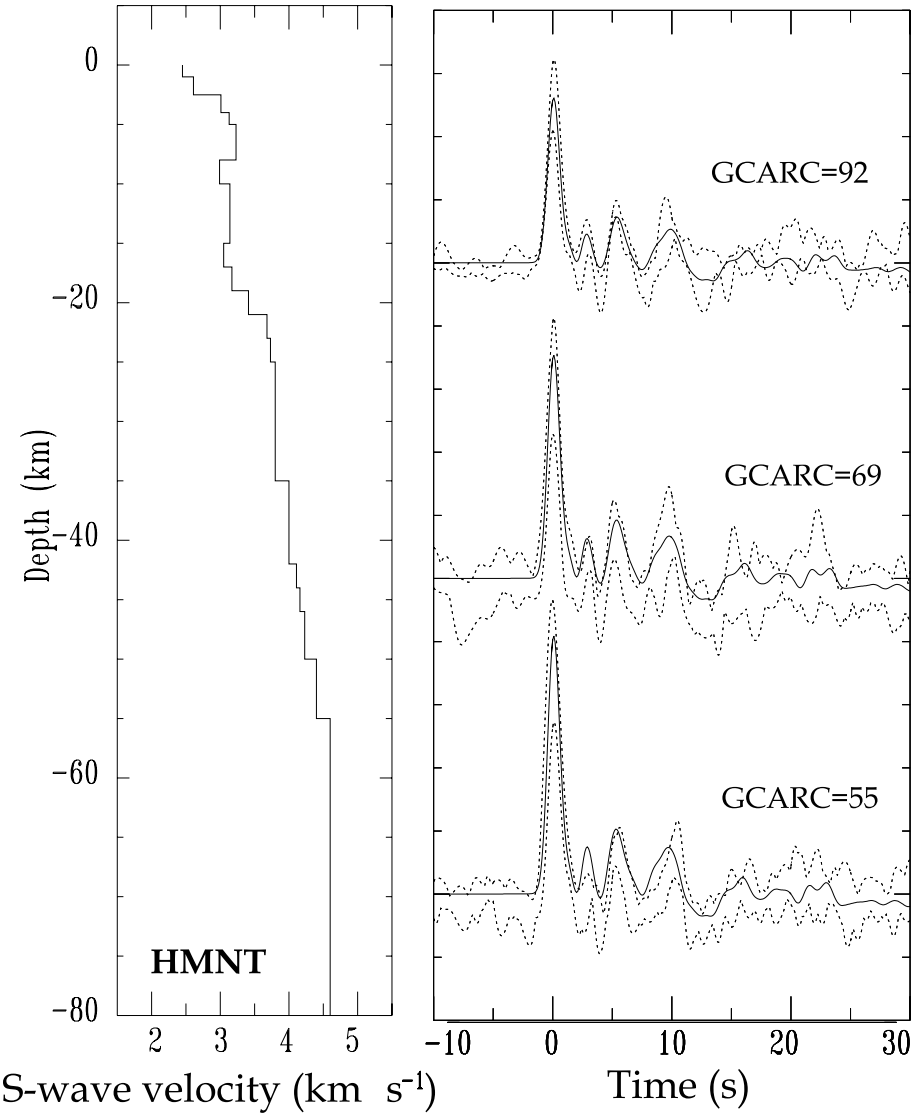

Figure 14. Crustal model and waveform fits for all-azimuth stacked receiver functions from station HMNT. Refer to Fig. 3 for plotting conventions. 'GCARC' is the average epicentral distance (in degrees) for the stacked group from station HMNT.

simple one-layered model with typical crustal and mantle velocities matches the position of this peak for a crustal thickness of ∼35 km.

5 DISCUSSION

Fig. 17 shows a summary of representative velocity–depth models for the Canadian High Arctic region. At most of the stations, it is possible to identify the depth to the Moho, which is modelled either as a sharp discontinuity or as a gradational transition occurring over 2–4 km. In several cases, where receiver functions have been modelled at different azimuths around the stations, different depths to the Moho have been identified, suggesting some degree of 3-D structure at depth. The depth to Moho is sampled both by *P*-to-*S* conversions (*Ps*) and by later reverberations. For a Moho depth of 30–40 km, the *Ps* arrivals originate from points between 5 and 15 km from the point vertically beneath the station, whereas the reverberations originate approximately 30–50 km away from the station. A Moho depth variation of up to 3 km with varying azimuth is modelled at some of the Arctic stations, suggesting that some variation exists over a 10–30 km lateral distance. Owing to the lateral sampling of *Ps* and reverberative phases, there is a possibility that a different Moho depth may be sampled by different phases in the same receiver function. However, the velocity–depth trade-off inherent in receiver function analysis, together with the restriction on vertical resolution owing to the wavelength of the incoming plane waves, suggests a likely error of $\sim \pm 2$ km for the depth to Moho in any receiver function modelled. Thus, the 3 km variation with azimuth lies within the bounds of the errors and is unlikely to present a significant problem in this study.

The stations lying on Precambrian granites and gneisses in the south and southeast of the Canadian Arctic region give rise to the simplest receiver functions with fairly laterally homogeneous structure compared with stations further north. At FRB, B1NU and SBNU, arrivals associated with the Moho are the most prominent features in the radial waveforms. Some crustal layering and upper-mantle structure is required to match the details of the receiver function waveforms but, in general, the crustal structures are relatively simple. Crustal thickness decreases from southeast to northwest on

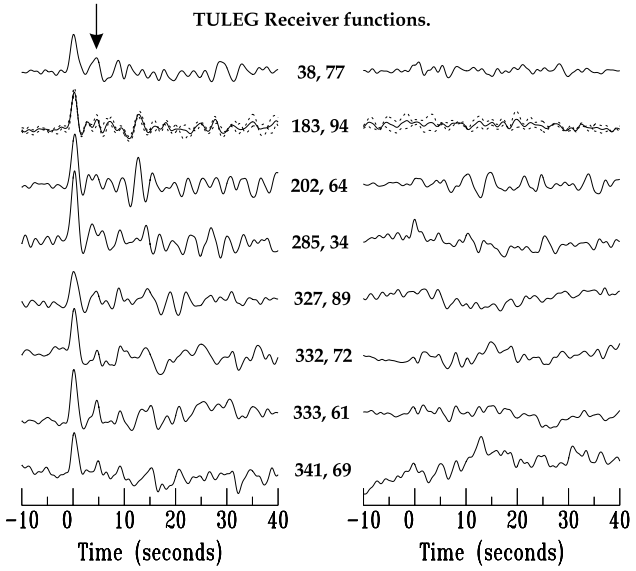

Figure 15. Receiver function data set for station TULEG on the west Greenland coast. Plotting conventions as for Fig. 2. The vertical arrow at the top of the plot indicates the position of the assumed Moho *P*-to-*S* conversion peak.

Baffin Island and towards the Boothia Peninsula, with the Moho depth at station SBNU close to the average for the Canadian Shield (e.g. Brune & Dorman 1963).

Both FRB and B1NU lie within a region of Early Proterozoic fold belts and igneous intrusions, probably associated with the Trans-Hudson Orogen (Corrigan *et al.* 2001). Some azimuthal variation in the receiver functions and crustal structures, and crustal layering beneath these two stations is therefore not surprising. FRB lies within the ∼1.86 Gyr old Cumberland Batholith, which extends over a large proportion of southern Baffin Island, though the station is relatively close to the Dorset Fold Belt in the southernmost part of the island. While B1NU lies within the boundaries of the Foxe Fold Belt, which is largely characterized by Early Proterozoic rocks (e.g. Hoffman 1988; Corrigan *et al.* 2001), the station itself lies on a dome of Archaean material, within a region of basin-and-dome structures arising from interference between two different periods of deformation (Corrigan *et al.* 2001). The substantial difference between the crustal structure south of B1NU and that southwest and northwest of the station may arise from the different tectonic regimes in the region. Between ∼39 and 46 km depth beneath B1NU, in the western crustal sections, a double discontinuity between crustal and mantle shear wave velocities was required to match the receiver function waveforms. The Trans-Hudson Orogen (and other orogens between North American Archaean provinces) has been interpreted

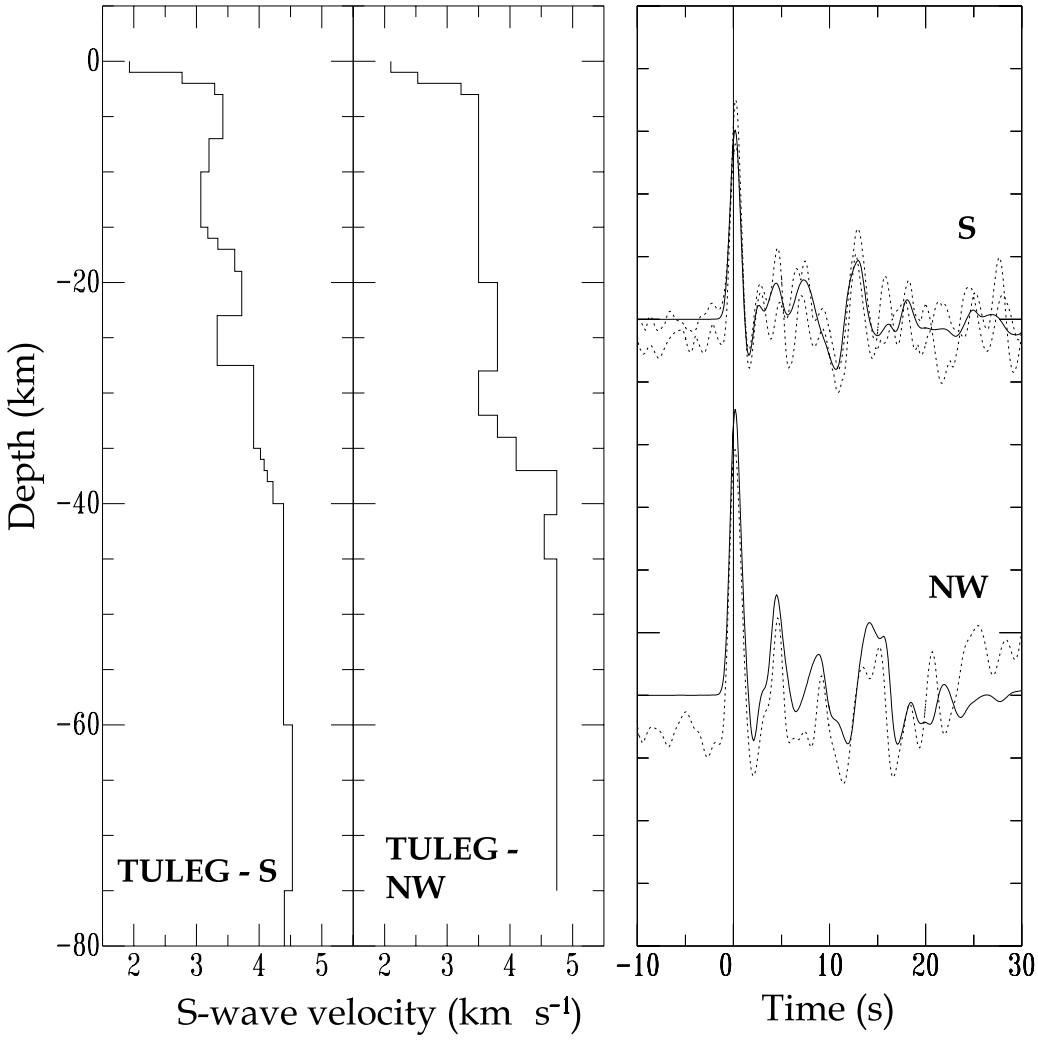

Figure 16. Crustal models and waveform fits for receiver functions from station TULEG. Refer to Fig. 3 for plotting conventions.

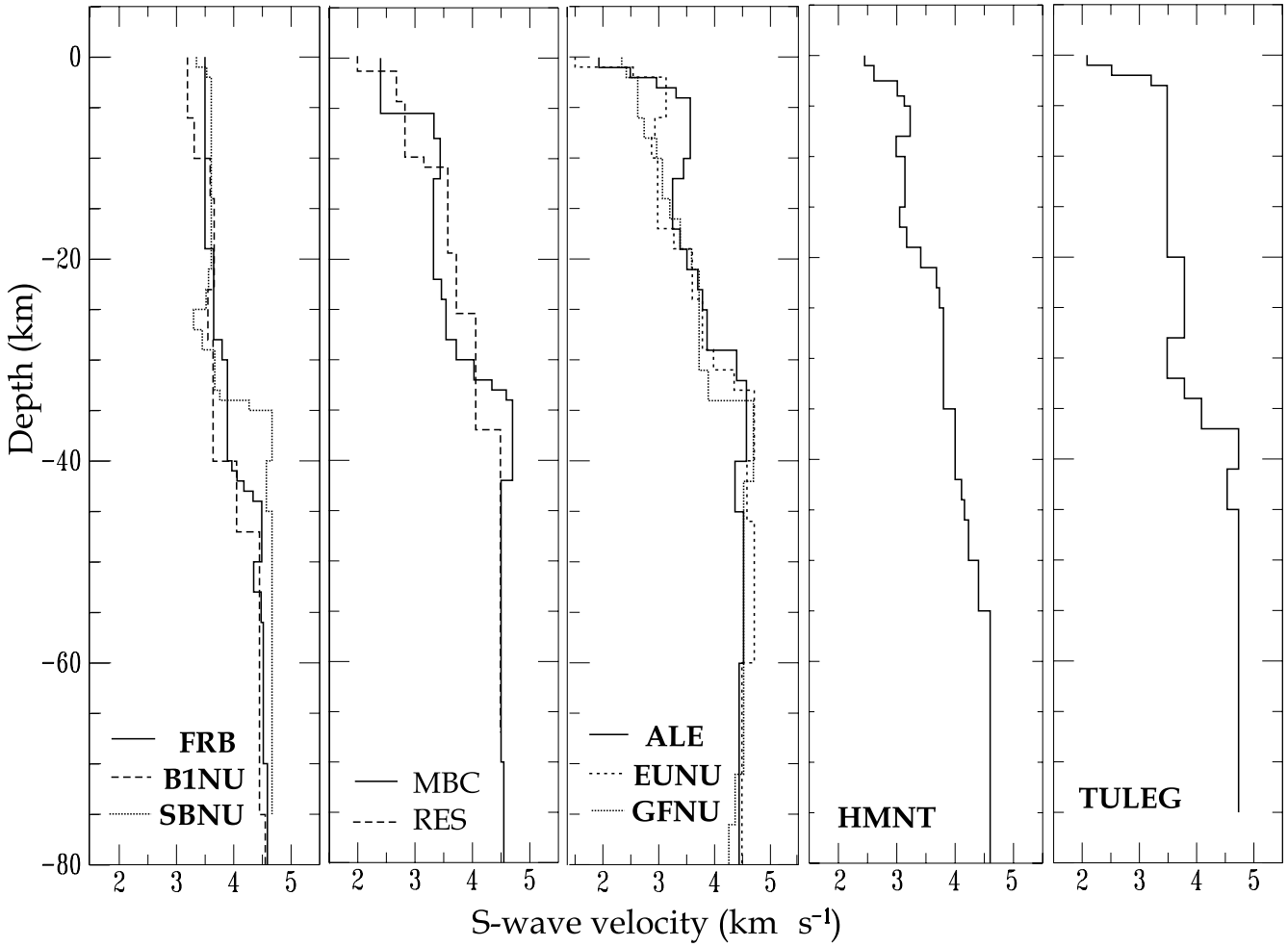

Figure 17. Summary plot of velocity–depth models from receiver function analysis. From left to right: Canadian Shield, Sverdrup Basin margins, Ellesmere Island, Holman, Thule (western Greenland).

as being associated with subduction regimes, therefore the structure observed in the receiver function models may represent a double Moho, associated with crust–mantle transitions beneath the orogen and the nearby Archaean lithosphere.

Laterally heterogeneous structure is a significant feature at stations in the northern and western parts of the Arctic islands, such as ALE, EUNU, RES and MBC. A dipping 5 km thick sedimentary layer beneath MBC obscures the details of the underlying crustal structure but, at ALE, EUNU and RES, the azimuthal variation in the radial receiver functions indicates large-scale 3-D features beneath the stations. The receiver functions are generally complex, requiring structure within both the crust and the uppermost mantle in order to match the waveforms. Some models also require low-velocity zones, though these are rarely modelled at more than one azimuthal group and may therefore be an artefact associated with scattering. The laterally heterogeneous structures are consistent with the complex tectonic history of the northern and northwestern Arctic region, which has been shaped by several orogenic events and sedimentary basin formation (e.g. Balkwill & Fox 1982; Thorsteinsson & Tozer 1970; Trettin 1991). For example, the strike of the 5 km depth dipping interface beneath MBC is similar to the direction of the tectonic trends in the region, where Franklinian fold belt structures border the Sverdrup basin.

Several of the receiver function models include sub-Moho structures in the form of velocity discontinuities well spaced in depth (e.g. RES south, EUNU) or discrete 5–10 km thick zones of high or low velocity (e.g. SBNU south, ALE south, TULEG northwest). Some of the layering may be accounted for by relicts of shallow subduction from the accretion of the provinces of the Canadian Shield, such as those inferred beneath the Slave craton by Bostock (1998). More recent tectonic events, such as orogenic episodes and the rifting associated with the formation of the Sverdrup Basin may also play a part in generating distinct structures within the uppermost mantle. Fault zones responsible for uplifting or depressing significant regions of the Arctic crust (such as the Boothia Uplift) may extend into the mantle, but it is unclear as to whether these might be imaged in single-station receiver function analysis.

The crustal thicknesses of 27–37 km across the northern Arctic archipelago are consistent with results from previous studies of the region. Moho depths of 32–42 km were inferred within the archipelago (e.g. Overton 1970; Forsyth *et al.* 1979; Sobczak & Overton 1984), and thinner crust (23–30 km) was inferred offshore of the Arctic coastal plain (e.g. Berry & Barr 1971; Asudeh *et al.* 1989; Forsyth *et al.* 1994), where the North American continental margin is rifted at the edge of the Arctic Ocean.

Holman (station HMNT) was the only one of the stations analysed where a Moho depth could not be inferred. Shear wave velocities typically associated with mafic lower crustal material (e.g. gabbros and granulites) lie at ∼35–55 km depth, above a half-space of velocity typical of continental uppermost mantle. The presence of mafic

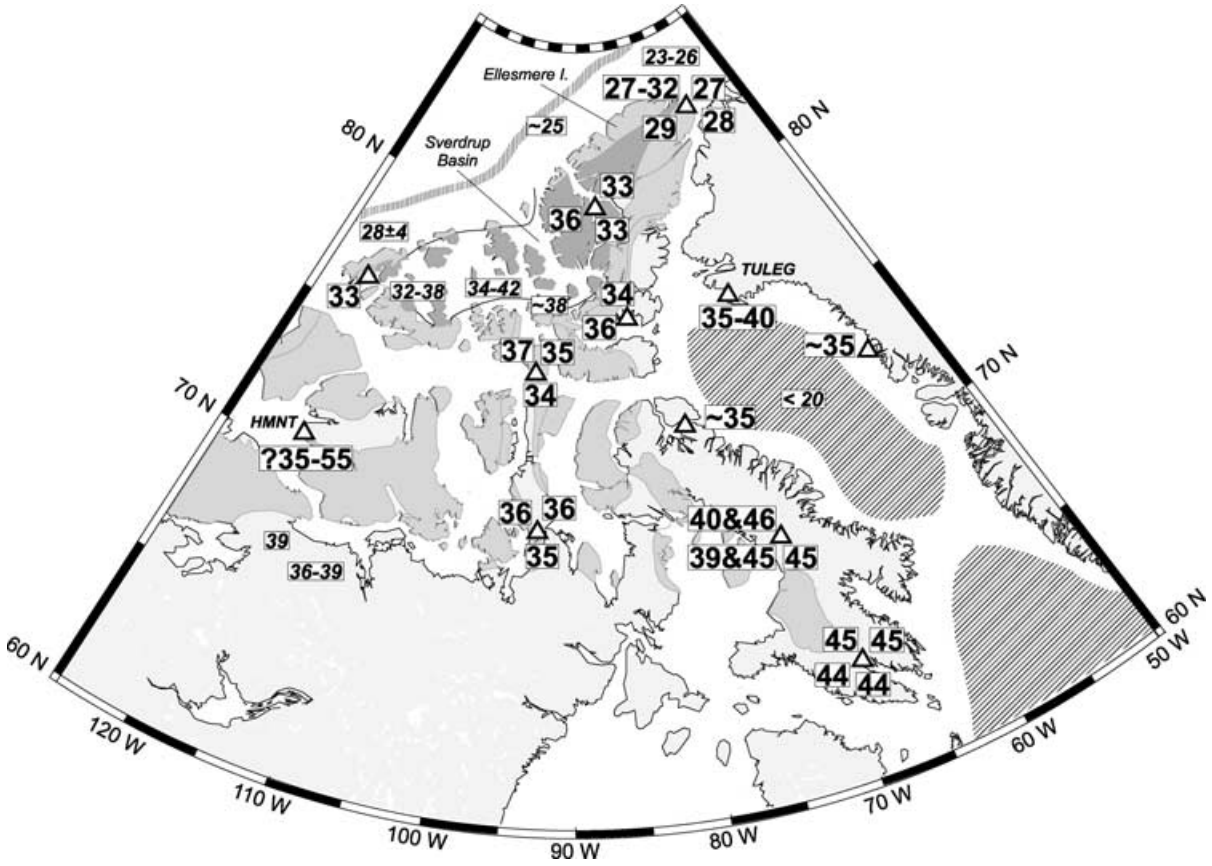

Figure 18. Map of crustal thicknesses across the Canadian High Arctic region. Bold font numbers clustered around white triangles (seismic stations) indicate crustal thicknesses obtained in this study. Numbers in italics (smaller font) indicate crustal thicknesses obtained from earlier studies such as refraction profiles and surface wave dispersion analyses. Crustal thicknesses in the Slave Province on the western mainland are taken from Bank *et al.* (2000). The hatched region indicates oceanic crust in Baffin Bay and the Labrador Sea (after Shih *et al.* 1988), and the hatched line to the north shows the position of the Arctic continental margin. The Canadian Shield is shaded in pale grey and the Sverdrup Basin is shaded in dark grey. The positions of stations HMNT and TULEG (mentioned by name in Fig. 17) are also marked.

material in the lower crust is consistent with the surface geology in the Holman area, where large outcrops of gabbro and diabase are common. (e.g. Geological Survey of Canada, map 900A, 1998) The results from the receiver function analysis agree with a surface wave study carried out by Wickens & Pec (1968), who modelled an intermediate-velocity layer ($V_s = 4.15$ km s^{-1}) between 35 and 50 km depth for the path between Mould Bay and Coppermine. The area around Holman lies at the focal point of the ∼1270 Myr old Mackenzie dyke swarm, north of the Coppermine River flood basalts (LeCheminant & Heaman 1989). The magmatism is believed to be associated with a mantle plume. It is possible that the layer of shear wave velocity 4.0–4.3 km s^{-1} beneath Holman is associated with mafic underplating arising from the plume activity *cf.* underplating beneath other large igneous provinces, such as the North Atlantic margins; e.g. White & McKenzie (1989).

6 SUMMARY

The crustal thickness across the Canadian High Arctic region and the west Greenland coast (Fig. 18) ranges from approximately 25 to 45 km (with the exception of the oceanic crust in Baffin Bay). In Canadian Shield regions, the crust has a relatively simple structure, with a prominent Moho. The northernmost part of the Shield, on the Boothia Peninsula, has a crustal thickness of ∼35 km but further south and east, on Baffin Island, the crust thickens to 40–45 km. Approximate Moho depths obtained for western Greenland show similar values of 35–40 km.

Away from the Shield, the crustal structure is more complex, with significant lateral heterogeneity, reflecting the tectonic structures of the region. Crustal thicknesses lie in the range 26–37 km, with the thinnest crust in the northernmost part of the Arctic archipelago. The shear wave velocities inferred from the crustal models suggest continental crust and uppermost mantle structure for most of the stations studied. However, in the southwestern part of the archipelago, anomalous shear wave velocities between 35 and 55 km depth are found, and there is an indication of anisotropic structure. The anomalous structure coincides with the focus of the Mackenzie dyke swarm and may represent lithosphere influenced by plume activity.

The crustal structure models developed from this study provide new information that can be used to refine the velocity models used in earthquake location for the region, thus increasing the knowledge of the current seismicity of the High Arctic and enabling more detailed seismic hazard studies to be carried out.

ACKNOWLEDGMENTS

The CHASME project is funded by the Comprehensive Nuclear Test Ban Treaty Office and the Geological Survey of Canada. FD is an NSERC visiting fellow funded by GSC. Allison Bent, John Adams, David McCormack (Principal Investigator for the

CHASME project), John Cassidy, Anya Reading and an anonymous reviewer gave helpful reviews of the manuscript. The CHASME project was carried out in collaboration with institutions in Denmark including the Danish National Survey & Cadastre, the Geological Survey of Denmark & Greenland, and the Danish Lithosphere Centre. We thank the Geological Survey scientists and technicians who deployed the CHASME seismic stations and the individuals in the Canadian and Greenland communities who assisted us during the initial fieldwork, and who have taken responsibility for data collection and instrument maintenance throughout the period of deployment. Seismic data for station B1NU were provided by David Snyder, Continental Geosciences Division, Geological Survey of Canada. Figs 1 and 18 were made using the GMT software of Wessel & Smith (1991). GSC contribution number 2001220.

REFERENCES

Ammon, C.J., 1991. The isolation of receiver effects from teleseismic *P* waveforms, *Bull. seism. Soc. Am.,* **81,** 2504–2510.

Ammon, C.J., Randall, G.E. & Zandt, G., 1990. On the non-uniqueness of receiver function inversions, *J. geophys. Res.,* **95,** 15 303–15 318.

Asudeh, I., Forsyth, D.A., Stephenson, R., Embry, A., Jackson, H.R. & White, D., 1989. Crustal structure of the Canadian polar margin: results of the 1985 seismic refraction survey, *Can. J. Earth Sci.* **26,** 853–866.

Balkwill, H.R. & Fox, F.G., 1982. Incipient rift zone, western Sverdrup Basin, Arctic Canada, in *Arctic Geology and Geophysics,* eds Embry, A.F. & Balkwill, H.R., Can. Soc. Petr. Geologists, memoir 8.

Balkwill, H.R., McMillan, N.J., MacLean, B., Williams, G.L. & Srivastava, S.P., 1990. Geology of the Labrador Shelf, Baffin Bay and Davis Strait, Chapter 7, in *Geology of the Continental Margin of Eastern Canada,* pp. 293–348, eds Kenn, M.J. & Williams, G.L., Geological Survey of Canada, Geology of Canada.

Bank, C.-G., Bostock, M.G., Ellis, R.M. & Cassidy, J.F., 2000. A reconnaissance teleseismic study of the upper mantle and transition zone beneath the Archean Slave craton in NW Canada, *Tectonophysics,* **319,** 151–166.

Basham, P.W., Forsyth, D.A. & Wetmiller, R.J., 1977. The seismicity of northern Canada, *Can. J. Earth Sci.* **7,** 1646–1667.

Berry, M.J. & Barr, K.G., 1971. A seismic refraction profile across the polar continental shelf of the Queen Elizabeth Islands, *Can. J. Earth Sci.* **8,** 347–360.

Berteussen, K.A., 1977. Moho depth determinations based on spectral ratio analysis of NORSAR long period *P* waves, *Phys. Earth planet. Inter.,* **15,** 13–27.

Bostock, M.G., 1998. Mantle stratigraphy and evolution of the Slave province, *J. geophys. Res.,* **103,** 21 183–21 200.

Brune, J. & Dorman, J., 1963. Seismic waves and earth structure in the Canadian Shield, *Bull. seism. Soc. Am.,* **53,** 167–210.

Buchbinder, G.G.R., 1963. Crustal structure in Arctic Canada from Rayleigh waves, *Trans. Roy. Soc. Canada,* **I,** 333–355.

Cassidy, J.F., 1992. Numerical experiments in broadband receiver function analysis, *Bull. seism. Soc. Am.,* **82,** 1453–1474.

Cassidy, J.F., 1995. A comparison of the receiver structure beneath stations of the Canadian National Seismograph Network, *Can. J. Earth Sci.,* **32,** 938–951.

Clayton, R.W. & Wiggins, R.A., 1976. Source shape estimation and deconvolution of teleseismic bodywaves. *Geophys. J. R. astr. Soc.,* **47,** 151–177.

Corrigan, D., Scott, D.S. & St-Onge, M.R., 2001. Geology of the northern margin of the Trans-Hudson Orogen (Foxe Fold Belt), central Baffin Island, Nunavut, Geological Survey of Canada, *Current Research 2001,* **C23,** p. 17.

Forsyth, D.A., Mair, J.A. & Fraser, I., 1979. Crustal structure of the central Sverdrup Basin, *Can. J. Earth Sci.* **16,** 1581–1598.

Forsyth, D.A., Argyle, M., Okulitch, A. & Trettin, H.P., 1994. New seismic, magnetic and gravity constraints on the crustal structure of the Lincoln Sea continent–ocean transition, *Can. J. Earth Sci.,* **31,** 905–918.

Helmberger, D. & Wiggins, R.A., 1971. Upper mantle structure of the Midwestern United States, *J. geophys. Res.,* **76,** 3229–3245.

Hoffman, P.F., 1988. United Plates of America, the birth of a craton: Early Proterozoic assembly and growth of Laurentia, *Ann. Rev. Earth planet Sci.,* **16,** 543–603.

Hoffman, P.F., 1990. Subdivision of the Churchill Province and extent of the Trans-Hudson Orogen, in *The Early Proterozoic Trans-Hudson Orogen of North America,* pp. 1–14, eds Lewry, J.F. & Stauffer, M.R., Geological Association of Canada, Special Paper 37.

Jackson, H.R., Keen, C.R. & Falconer, R.K.H., 1979. New geophysical evidence for sea-floor spreading in central Baffin Bay, *Can. J. Earth Sci.,* **16,** 2122–2135.

Jones, C.H. & Phinney, R.A., 1998. Seismic structure of the lithosphere from teleseismic converted arrivals observed at small arrays in the southern Sierra Nevada and vicinity, California, *J. geophys. Res.,* **103,** 10 065–10 090.

Keen, C.E., Barrett, D.L., Manchester, K.S. & Ross, D.I., 1972. Geophysical studies in Baffin Bay and some tectonic implications, *Can. J. Earth Sci.,* **9,** 239–256.

Kennett, B.L.N., 1983. *Seismic Wave Propagation in Stratified Media,* Cambridge University Press, Cambridge.

Kerr, J.W., 1977. Cornwallis Fold Belt and the mechanism of basement uplift, *Can. J. Earth Sci.* **14,** 1374–1401.

Langston, C.A., 1977. The effect of planar dipping structure on source and receiver responses for constant ray parameter, *Bull. seism. Soc. Am.,* **67,** 1029–1050.

Langston, C.A., 1979. Structure under Mount Rainier, Washington, inferred from teleseismic body waves, *J. geophys. Res.,* **84,** 4749–4762.

LeCheminant, A.N. & Heaman, L.M., 1989. Mackenzie igneous events, Canada: Middle Proterozoic hotspot magmatism associated with ocean opening, *Earth planet. Sci. Lett.,* **96,** 38–48.

Levin, V. & Park, J., 1998. *P–SH* Conversions in layered media with hexagonally symmetric anisotropy: a cookbook, *Pure appl. Geophys.,* **151,** 669–697.

Lewry, J.F. & Collerson, K.D., 1990. The Trans-Hudson Orogen: extent, subdivision and problems, in *The Early Proterozoic Trans-Hudson Orogen of North America,* pp. 1–14, eds Lewry, J.F. & Stauffer, M.R., Geological Association of Canada, Special Paper 37.

Okulitch, A.V., Packard, J.J. & Zolnai, A.I., 1991. Late Silurian—Early Devonian deformation of the Boothia Uplift. Chapter 12, in *Geology of the Innuitian Orogen and Arctic Platform of Canada and Greenland,* ed. Trettin, H.P., Geological Survey of Canada, Geology of Canada, p. 569.

Overton, A., 1970. Seismic refraction surveys, western Queen Elizabeth Islands and Polar continental margin, *Can. J. Earth Sci.* **7,** 346–365.

Randall, G.E., 1989. Efficient calculation of differential seismograms for lithospheric receiver functions, *Geophys. J. Int.* **99,** 469–481.

Sander, G.W. & Overton, A., 1965. Deep seismic refraction investigation in the Canadian Arctic archipelago, *Geophysics,* **24,** 87–96.

Sheriff, R.E. & Geldart, L.P., 1982. *Exploration Seismology Volume 1: History, Theory and Data Acquisition,* Cambridge University Press, Cambridge.

Shih, K.G., Kay, W., Woodside, J., Jackson, R., Adams, J., Drysdale, J., Bell, J.S. & Podrouzek, A.J., 1988. *Crustal Thickness, Seismicity and Stress Orientations of the Continental Margin of Eastern Canada,* Geological Survey of Canada, Map 1710A.

Snyder, D., Asudeh, I., Darbyshire, F. & Drysdale, J., 2002. Field-based feasibility study of teleseismic surveys at high northern latitudes, Northwest Territories and Nunavut, Geological Survey of Canada, *Current Research 2002,* **C03,** p. 10.

Sobczak, L.W. & Overton, A., 1984. Shallow and deep structure of the western Sverdrup Basin, arctic Canada, *Can. J. Earth Sci.,* **21,** 902–919.

Thorsteinsson, R. & Tozer, E.T., 1970. Geology of the Arctic Archipelago, in *Geology and Economic Minerals of Canada, Geol. Surv. Can., Econ. Geol. Rept.,* pp. 548–590, ed. Douglas, R.J.W.

Trettin, H.P., 1991. Introduction; Chapter 1, in, *Geology of the Innuitian Orogen and Arctic Platform of Canada and Greenland,* ed. Trettin, H.P., Geological Survey of Canada, Geology of Canada, p. 569.

Wessel, P. & Smith, W.H.F., 1991. Free software helps map and display data, *EOS, Trans. Am. geophys. Un.,* **72,** 441, 445–446.

Wetmiller, R.J., 1974. Crustal structure of Baffin Bay from the earthquake-generated L_g phase, *Can. J. Earth Sci.,* **11,** 123–130.

White, R.S. & McKenzie, D.P., 1989. Magmatism at rift zones: the generation of volcanic continental margins and flood basalts, *J. geophys. Res.,* **94,** 7685–7729.

Wickens, A.J., 1971. Variations in lithospheric thickness in Canada, *Can. J. Earth Sci.,* **8,** 1154–1162.

Wickens, A.J. & Pec, K., 1968. A crust–mantle profile from Mould Bay, Canada, to Tucson, Arizona, *Bull. seism. Soc. Am.,* **58,** 1821–1831.

Zelt, B.C. & Ellis, R.M., 1999. Receiver-function studies in the Trans-Hudson Orogen, Saskatchewan, *Can. J. Earth Sci.,* **36,** 585–603.

Ziegler, P.A., 1988. Evolution of the Arctic—North Atlantic and the western Tethys, *AAPG Memoir,* **43** p. 198.